University of Thessaly
School of Health Sciences
Department of Biochemistry and Biotechnology

Mechanisms of post-transcriptional regulation of gene expression in dementia

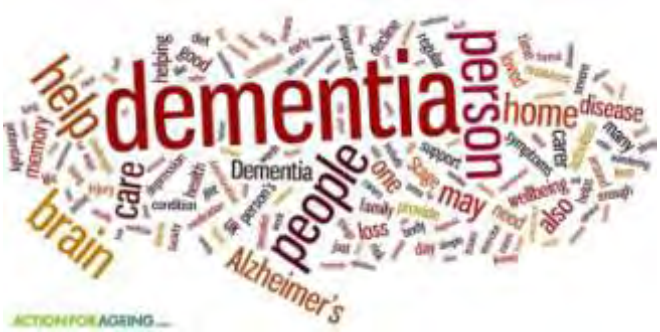

Μηχανισμοί μετα-μεταγραφικής ρύθμισης της γονιδιακής έκφρασης στην άνοια

Komini Ourania

Trento, Italy 2014

First and foremost, I have to thank my research supervisor Dr Michela Alessandra Denti. Without her assistance and dedicated involvement in every step throughout the process, this thesis would have never been accomplished. I would like to thank you very much for your support and understanding over my period in your laboratory.

I would also like to show gratitude to my committee, my co- supervisor Dr Nikolaos Balatsos and the member Dr Emily Zifa. Special thanks to Dr Nikolaos Balatsos for his help and support over the last four years at the Department of Biochemistry and Biotechnology, and for his assistance in the process of the Erasmus project.

I would like to thank all my professors teaching me enthusiasm, ethics and imagination giving me the best prospects to achieve my dreams and become a right scientist. I would like to thank also the Erasmus program giving me the opportunity to study abroad and accomplish my thesis.

I would like to thank Francesca Fontana, phD student at the laboratory of RNA Biology and Biotechnology for her help and her patience to teach me techniques and how to think to solve problems in the workflow of an experiment.

Getting through my dissertation required more than academic support, and I have many, many people to thank for listening to and, at times, having to tolerate me over the past three years. I cannot begin to express my gratitude and appreciation for their friendship.

Most importantly, none of this could have happened without my family (my father, my mother and my brother). They offered their encouragement through phone calls every week – despite my own limited devotion to correspondence. It would be an understatement to say that, as a family, we have experienced some ups and downs in the past four years. Every time I was ready to quit, you did not let me and I am forever grateful. This dissertation stands as a testament to your unconditional love and encouragement.

Supervisor	**Co- Supervisor**	**Member**
Dr Michela A. Denti	**Dr Nikolaos Balatsos**	**Dr Emily Zifa**

Table of Contents

1. Abstract

Frontotemporal Lobar Degeneration (FTLD) is a neurodegenerative disease associated with different patterns of atrophy of the frontal and temporal lobes of the brain. The pathology is characterized by an early onset and mainly by changes in behavior and personality, with aphasia and language difficulties. Many studies have shown that mutations in some genes could cause FTLD. Among the genes that are involved, *MAPT* mutations are the most common in FTD population. The second most common gene is *GRN* which represents the 5- 10% of mutations in FTLD. *GRN* is located in chromosome 17q21 and encodes for progranulin, which is a secreted glycoprotein. Progranulin can be proteolytically cleaved, resulting in small peptides called granulins. Progranulin plays a role in multiple biological functions, including promoting cell cycle progression and survival, proliferation and migration of several cell types, transcriptional repression, embryogenesis and inflammation. It is shown that the presence of mutations in *GRN* results in a reduction of the levels of progranulin that is relevant for the onset of FTLD. All the mutations found in the coding region of *GRN* cannot explain the heterogeneous panel of the pathological characteristics observed in the disease state. This project aims at studying the mechanism of post- transcriptional regulation of *GRN* gene played by miRNA. MicroRNAs are a class of ~22 nt non- conding RNAs that control diverse biological functions in animals, plants and unicellular eukaryotes by promoting degradation or inhibition of translation of target mRNAs. We investigated the regulation effect of several microRNAs on the GRN 3'UTR. We found that miR-659 and miR-608 have the strongest regulation effect. Understanding that microRNAs regulate the expression of progranulin may pave the way to new diagnostic tools and treatments for FTLD.

2. Περίληψη

Η μετωποκροταφική άνοια (ΜΚΑ) είναι μια νευροεκφυλιστική νόσος που σχετίζεται με διαφορετικά πρότυπα ατροφίας του μετωπικού ή και του κροταφικού λοβού του εγκεφάλου. Η παθολογία της νόσου χαρακτηρίζεται από πρώιμη έναρξη και κυρίως από αλλαγές στην συμπεριφορά και στην προσωπικότητα του ασθενούς, καθώς και από αφασία και γλωσσικές δυσκολίες. Πολλές έρευνες έδειξαν ότι μεταλλάξεις σε κάποια γονίδια θα μπορούσαν να προκαλέσουν την μετωποκροταφική άνοια. Μεταξύ όλων των γονιδίων που εμπλέκονται στην εμφάνιση της νόσου, οι μεταλλάξεις στο γονίδιο *MAPT* είναι οι πιο συχνές στον πληθυσμό με ΜΚΑ. Το δεύτερο πιο συχνό γονίδιο με μεταλλάξεις είναι το γονίδιο *GRN* που εκφράζει το 5-10% των μεταλλάξεων στην ΜΚΑ. Το γονίδιο *GRN* χαρτογραφείται στο χρωμόσωμα 17q21 και κωδικοποιεί για την προγρανουλίνη, η οποία είναι μια εκκρινόμενη γλυκοπρωτεΐνη. Η προγρανουλίνη μπορεί να υποστεί πρωτεολυτική πέψη έχοντας ως αποτέλεσμα την δημιουργία μικρών πεπτιδίων που ονομάζονται γρανουλίνες. Η προγρανουλίνη διαδραματίζει σημαντικό ρόλο σε διάφορες βιολογικές λειτουργίες, συμπεριλαμβανομένου της προώθησης του κυτταρικού κύκλου και της επιβίωσης, της εμβρυογένεσης, της φλεγμονής, της διαφοροποίησης και της μετανάστευσης διάφορων κυτταρικών τύπων και της καταστολής της μεταγραφής,. Έχει δειχθεί ότι η παρουσία μεταλλάξεων στο γονίδιο *GRN* συντελεί στην μείωση των επιπέδων της προγρανουλίνης, το οποίο σχετίζεται με την εμφάνιση της ΜΚΑ. Όλες οι μεταλλάξεις που έχουν βρεθεί στην κωδική περιοχή του γονιδίου *GRN* δεν μπορούν να εξηγήσουν την ετερογένεια των παθολογικών χαρακτηριστικών που παρατηρούνται κατά την διάρκεια της νόσου. Αυτή η εργασία έχει ως στόχο την μελέτη του μηχανισμού της μετα-μεταγραφικής τροποποίησης του γονιδίου *GRN* από τα miRNAs. Τα microRNAs είναι μια κατηγορία μη κωδικών RNAs μήκους ~ 22 νουκλεοτιδίων τα οποία μπορούν και ελέγχουν διάφορες βιολογικές λειτουργίες σε ζώα, φυτά και μονοκύτταρους ευκαρυώτες, προωθώντας την αποικοδόμηση ή την αναστολή της μετάφρασης των mRNAs στόχων. Εξετάσαμε την επίδραση κάποιων microRNAs στην ρύθμιση της 3’ UTR του γονιδίου *GRN* και παρατηρήσαμε πως, ισχυρότερη επίδραση έχουν τα miR-659 και miR-608. Η κατανόηση ότι τα microRNAs ρυθμίζουν την έκφραση της προγρανουλίνης μπορεί να ανοίξει το δρόμο για νέα διαγνωστικά εργαλεία και θεραπείες για την ΜΚΑ.

3. Introduction

3.1. Frontotemporal Lobar Degeneration

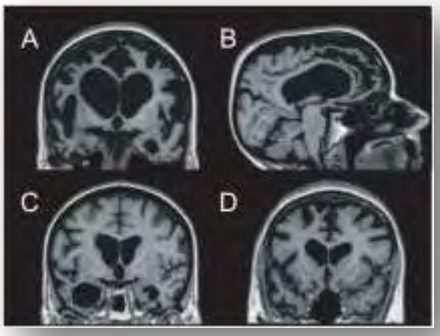

Figure 1 MIR findings in FTLD. A, B behavioral dementia, C semantic aphasia, D PNFA.[41]

Frontotemporal Lobar Degeneration (FTLD) is a group of neurodegenerative diseases associated with diverse patterns of atrophy of the frontal and temporal lobes of the brain[1]. The age of onset is around 50 – 70 years in 75-80% of the patients. Frontotemporal Lobar Degeneration is the second most common cause of dementia. It includes a large group of neurodegenerative disorders characterized mainly by changes in behavior and personality, with aphasia and language difficulties[2].

Classification of FTLD patients appears to be complicated due to heterogeneous clinical symptoms observed in patients and the overlaps between the neurodegenerative mechanisms[34]. Patients with FTLD can be characterized through their clinical symptoms in three groups: a behavioral variant (bvFTD) and two language variants (semantic dementia and progressive non fluent aphasia). One characterization can be based on the proteinopathies. So, FTLD is divided in the group of FTLD-tau, FTLD- FUS, and FTLD-TDP. The Figure 2 presents the classification of FTLD. Molecular genetic studies have identified five genes that, when they are mutated cause FTLD. The genes that are involved are *MAPT*, *GRN*, *C9orf72*, *VCP*, *CHMP2B, TDP- 43 and FUS* as observed in figure 2.

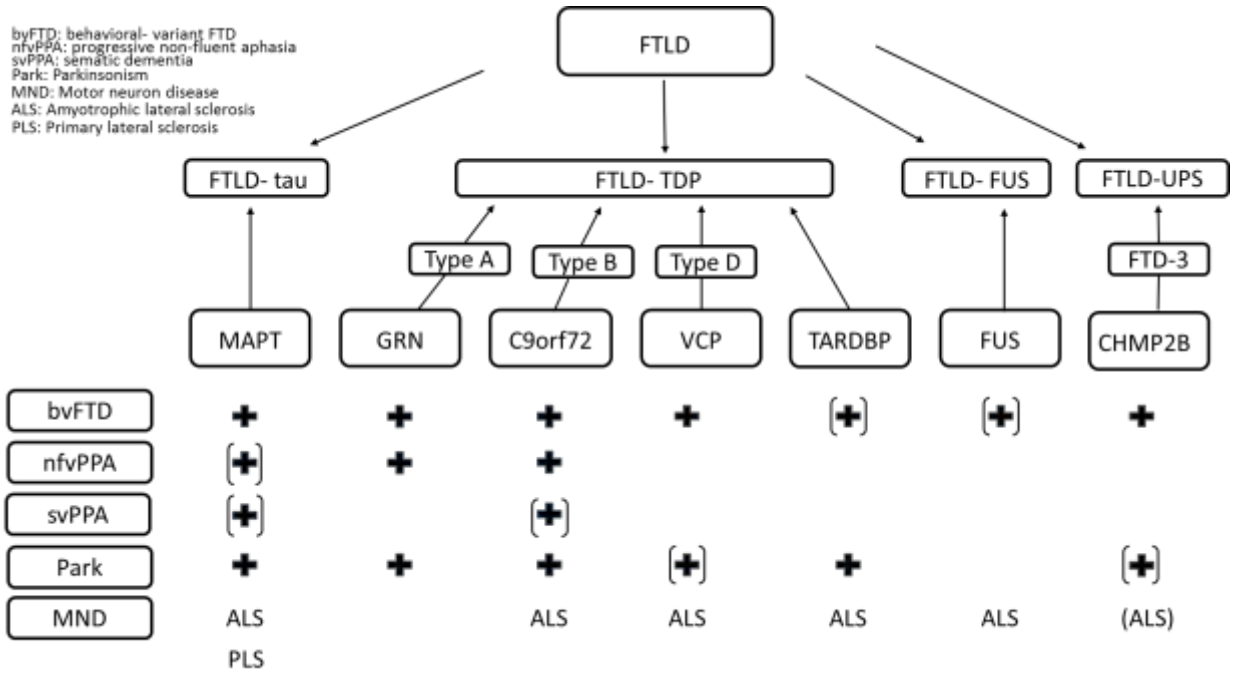

Figure 2 Classification of FTLD.

MAPT gene is the first significant genetic linkage found in FTLD families. It is located at chromosome 17q21 and encode tau protein[2]. Tau protein in neurons binds to axonal microtubules and promotes microtubule stabilization[5]. Until now 44 different mutations found in *MAPT* were reported as the cause of the 5-20% of FTLD families[6].

A noncoding GGGGCC hexanucleotide repeat has been identified in ***C9orf72***[7]. In normal population the size of this hexanucleotide repeat ranges from 3 to 25 units, while in patients it is expanded to 60 units and more[2]. The *C9orf72* encodes for an ubiquitously expressed protein with unknown function[7].

In ***VCP*** gene 17 mutations have been found in 41 independent families[8]. *VCP* is located at chromosome 9p21[9] and encodes a ubiquitously expressed member of a family of ATPases[2]. The ATPases are associated with a wide variety of cellular functions through interactions with adaptor proteins[10].

CHMP2B gene is located at chromosome 3p13- 3p12. It is mainly expressed in neurons of all major brain regions. It encodes the ESCRT- III complex, the endosomal sorting complex required for transport. Its role is in protein degradation pathway.

TARDBP gene is located at chromosome 1p36.2. It encodes TDP-43, a 414 aminoacid protein, and consists of five coding and non-coding exon[11]. TDP-43 is an RNA- binding protein that forms heterogeneous nuclear ribonucleoprotein complexes (hnRNP), and plays a role in RNA processing activities of several cellular functions[2].

FUS gene is located at chromosome 16p11.2. It encodes FUS, a 526 aminoacid protein, and is a member of the hnRNP family. It is implicated in numerous cellular processes, including RNA and miRNA processing[12].

The second most common cause of FTLD is the presence of mutations in ***GRN***[13] and we decided to concentrate our attention on its post- transcriptional regulation. *GRN* is located at the chromosome 17q21[14]. So far 69 different mutations have been reported in 231 families[2].

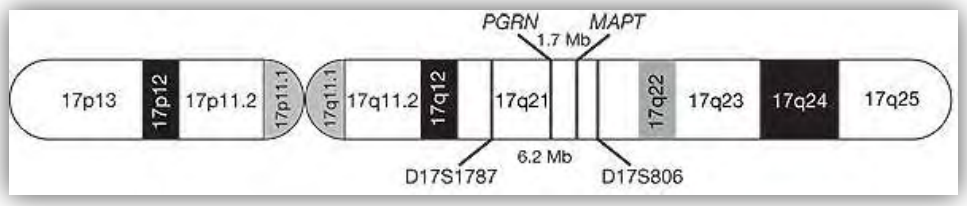

Figure 3 Schematic presentation of chromosome 17[28]

3.2. *GRN* and Progranulin

GRN is a gene located in chromosome 17q21 and encodes a protein, progranulin. *GRN* is composed of 13 exons[15] with the presence of a non- coding exon 1. Progranulin is translated as 593 amino acid, 68.5 kDa cysteine- rich protein. It is highly glycosylated and secreted as a protein of 88 kDa[16]. The structure of progranulin consist of four stacked β- hairpins in a twisted ladder formation, with the help of disulfide bridges forming a central rod-like structure[17] .

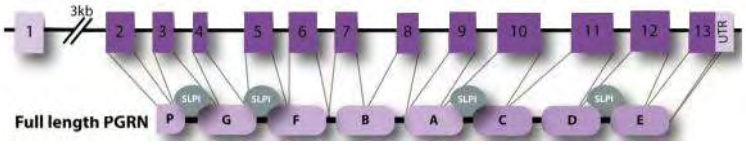

Figure 4 Schematic presentation of GRN and the full length of the PGRN. SLPI is the secretory leucocytes protease inhibitor, which prevent the cleavage of full length of PGRN by elastase.[15]

The protein is composed of intra-linked granulin peptides. The peptides are being subsequently cleaved by protease into individual peptides, each composed of cysteine repeat motifs[15]. Progranulin (PGRN), also known as granulin –epithelin precursor is a protein that plays a role in multiple biological functions, including promoting cell cycle progression and survival[18,19,20], proliferation and migration of several cell types, transcriptional repression[21], embryogenesis[22] and inflammation[18]. Studies have shown that progranulin plays a role in wound-healing response [13]. Progranulin is expressed in many tissues of the body, and in particular in epithelial and hematopoietic cells[13]. Usually progranulin is highly expressed in cells with high mitotic rate such as skin epithelium and expressed at low levels in cells with low mitotic rate[23]. Exception of this rule is the epididymal cells which have low mitotic rate but high level of progranulin[23]. Less is known about the effect and the role of progranulin in CNS.

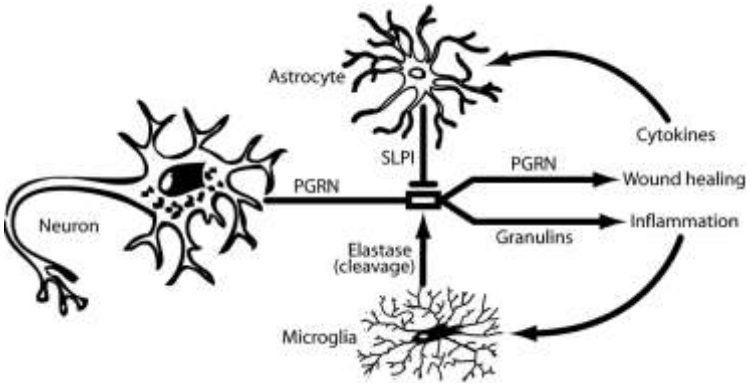

Figure 5 Potential role of GRN in CNS[10]

The scheme in Figure 5 shows the potentials effects of progranulin in CNS. As shown in the picture, in the case of inflammation PGRN can be cleaved by elastase and other type of protease released by microglia. The cleavage of the PGRN can cause additional inflammatory events.

Granulins have an inflammatory role while, the progranulin has an anti-inflammatory role with the help of cytokines. On the other hand, astrocytes secrete proteins that inhibit the cleavage of PGRN. In case of inflammation the cytokines activate the astrocytes and promote the secretion of SLPI. SLPI causes the reduction of the cleavage of PGRN which promote the wound healing pathways[13].

3.3. Progranulin mutations

It has been shown that mutations in *GRN* can cause FTLD – TDP proteinopathy type A[2]. Clinicopathologies studies have shown that FTLD-TDP type A is most common with a percentage of 41- 49% of the cases[2,24]. Until now, 69 different mutations have been identified in 231 families. The mutations include frameshift, nonsense, and missense mutations[25]. Mutations have been identified also in noncoding regions, such as promoters, introns, 3'-5' UTR. The mutations are loss of function, that cause a reduction of the protein level and lead to haplo-insufficiency[26,27,28]. Recent studies show a frequency of *GRN* mutations of 5-10% in FTD population[13].

3.4. miRNAs : Biogenesis and mechanism

MicroRNAs are a class of ~22 nt non- conding RNAs that control diverse biological functions in animals, plants and unicellular eukaryotes by promoting degradation or inhibition of translation of target mRNAs[29]. They are transcribed in time and tissue

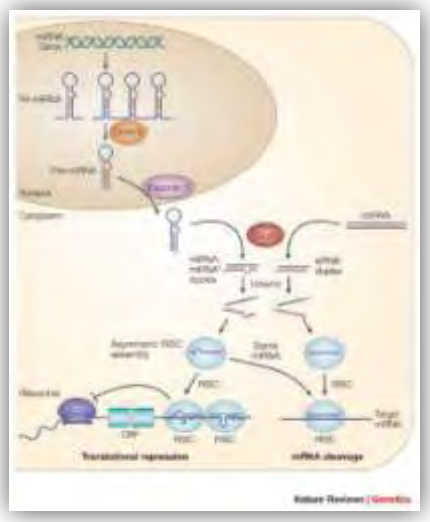

Figure 6 miRNA Biogenesis[42]

specific manner.

Commonly, miRNAs are transcribed from intragenic or intergenic DNA regions by the enzyme RNA polymerase II. The transcripts is 1-3kb long and is called pri-miRNA[30]. Subsequently the RNase complex, the RNase III Drosha and its cofactor DGCR8 perform an endonucleolytic cleavage of the pri-miRNA[31]. This cleavage produce a

hairpin structure named pre-miRNA with a length of 70-100 nt. Afterwards, the pre-miRNA is transported from the nucleus to the cytoplasm by Exportin-5. Dicer, another RNase III enzyme, helps the maturation of pre-miRNA to a double-stranded miRNA of variable length (~20-25nt) in the cytosol [32]. The guide strand or mature miRNA is joined into RISC, and also the other miRNA called miRNA* can have an effect [33,34]. In the RISC complex, the miRNA binds to its target mRNA and causes target silencing with the help of Argonaute (AGO). The miRNA targeting is specified by base- pairing between nucleotides from positions 2 to 8 in the miRNA seed. The binding of the miRNA is mainly localized in the 3'-UTR of the target mRNA[35], however it can also binds the coding and the 5' UTR regions. When there is a perfect complementarity between miRNA and mRNA, the RISC complex induces mRNA degradation, whereas imperfect miRNA- mRNA complementarity results in translation inhibition[35]. The complex of imperfect binding (miRNA/mRNA) could be translocated to cytoplasmic processing bodies (P-bodies) where untranslated mRNAs are stored and degraded [36].

3.5. miRNAs and progranulin

As described previously, miRNAs can regulate the translation and stability of the mRNAs and as a result the levels of the proteins. Changes in the miRNA expression profiles and polymorphisms affect the interaction between miRNAs and their targets [37]. 3 different miRNAs are reported in literature that could regulate the expression level of *GRN*. In 2008 Rosa Rademakers and colleagues discovered that miR-659 can be a possible regulator of *GRN*. The scientists found that a common genetic variant (rs5848), which is located in a binding site region of miR-659 localized in the 3'UTR of *GRN*, increases the risk of developing FTLD-TDP, type A. The presence of the SNP creates a stronger binding of the miR-659 that cause a strong down-regulation and suppressed translation of *GRN* mRNA[38] .

In silico analysis has shown the pairing of miR-659 to the predicted binding site in the 3' UTR of *GRN,* as represented in figure 7. In the (A)

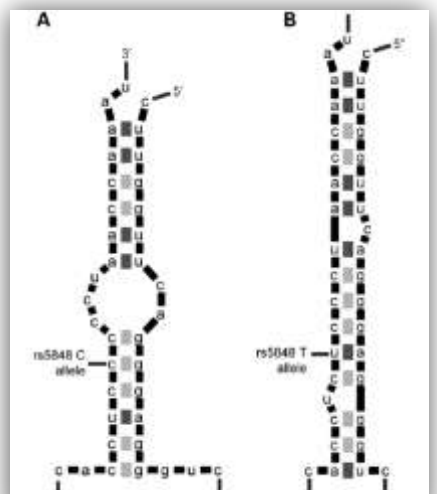

Figure 7 In silico analysis of the base pairing of the miR-659 in the 3' UTR[38]

scheme is base pairing in the presence of wild type C-allele at the site of the common genetic variant (rs5848) and in the (B) scheme is illustrated the base pairing in the presence of the SNP (T-allele) at the rs5848[38]. In the presence of the SNP the base pairing is stronger between the miR-659 and the 3' UTR than in the presence of the wild type allele.

Two years later other two microRNAs were found to regulate the expression of the human progranulin, miR-29b and miR- 107. It is reported that the miR-29b interacts directly with the 3' UTR of *GRN*, and regulates its expression[39]. Although the 3' UTR sequences tend to drift rapidly during evolution[35], the binding sites for miR-29b in the 3' UTR of *GRN* seem to be highly conserved in mammals[39]. miR-107 was also shown to have a regulative role for *GRN*[40]. miR-107 appears to target *GRN* in the open reading frame of the mRNA.

4. Aim of the study

This study is a part of a larger project which has as an aim to develop therapeutic strategies for the treatment of Frontotemporal lobar degeneration, due to the fact there is no effective treatment for this type of disease. One of the main causes associated with the disease is the mutations in *GRN*. In this project we studied the mechanism of post-transcriptional regulation of *GRN* mediated by microRNAs. MicroRNAs have the capability to act at the post-transcriptional level, targeting the mRNA. Bioinformatics predictions show that different miRNAs can bind on the 3'UTR of *GRN*, such as miR-615-5p, miR-939, miR-659, and miR-608. The hypothesis we tested was a role of the identified miRNAs in post-transcriptional regulation of *GRN*. We transfected in HeLa cell line two plasmids, one for the overexpression of the miRNAs of our interest and one that contains the luciferase cDNA followed by the *GRN* 3' UTR. We observed the effect of miRNAs through Luciferase Assay, ELISA Assay and Western Blot. We also monitored the over-expression of the miRNAs under study by Real Time PCR. The presence of miRNAs and the subsequent recognition of the target site should result in blocking the translation of messenger RNA and therefore lower the levels of the expression of Luciferase and the protein levels of progranulin. The study was part of my ERASMUS scholarship and was conducted at the Laboratory of RNA Biology and Biotechnology of the University of Trento, Italy.

5. Materials and Methods

5.1. Plasmids

Different bioinformatics tools such as PITA algorithm, TargetScan, Targetprofiler were used to predict the best putative microRNAs that can bind the 3' UTR of *GRN*. The microRNAs with the best score in terms of free binding energy and site accessibility were selected for the following experiments. Previous work in the laboratory leaded to the production of over-expressing vectors of the selected microRNAs and different specific reporter vector containing the full length *GRN* 3' UTR and specific fragments of the *GRN* 3' UTR with different binding sites for putative microRNAs.

In figure 8 is presented the full length of *GRN* 3' UTR of 304bp, the fragments in which the 3' UTR of *GRN* was divided and relative positions of the miRNA binding sites. The Part I of the *GRN* 3'UTR of 114 bp was also divided in two smaller

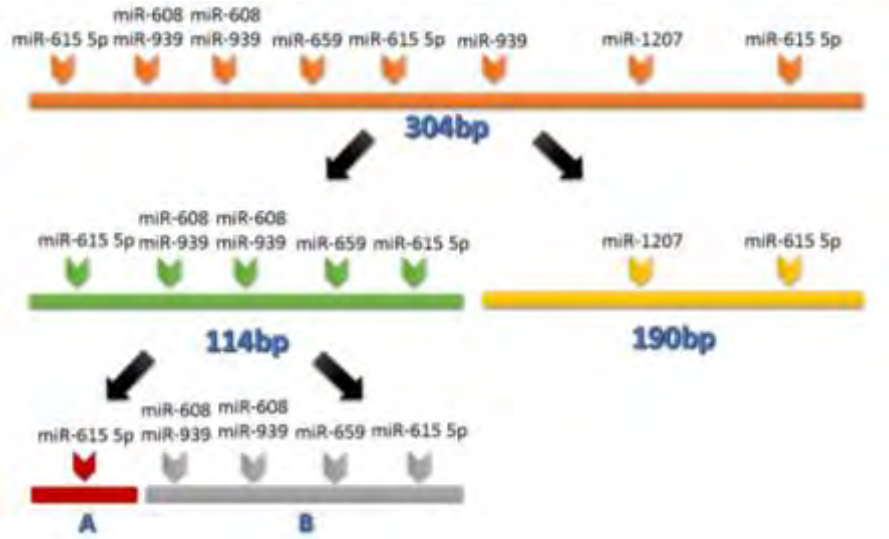

Figure 8 Schematic representation of miRNAs binding sites on the GRN 3'UTR and its division in fragments

fragments (fragment A and fragment B).

The pmirGLO Dual Luciferase miRNA Target Expression Vector from Promega was used for cloning of th *GRN* 3' UTR and the different fragments. In figure 9 is shown a

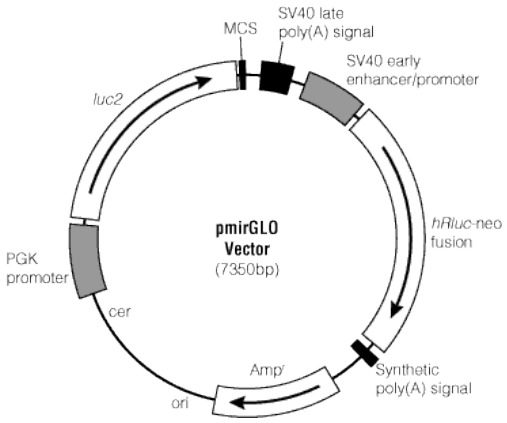

Figure 9 Schematic representation of pmirGLO Vector

schematic representation of the vector.

The vector contains the human phosphoglycerate kinase (*PGK*) promoter which provides low translational expression. It contains the firefly luciferase reporter gene (*luc2*) used as the primary reporter to monitor mRNA regulation. The multiple cloning site (*MCS*) located on the 3' of the firefly luciferase reporter gene (*luc2*) is used to clone the 3' UTR of interest through the use of specific restriction sites. The vector contains a SV40 late poly (A) signal sequence, which is positioned downstream of luc2 to provide efficient transcription termination and mRNA polyadenylation, and a synthetic poly (A) signal/ transcription stop site. Under the control of another promoter called SV40 early enhancer/promoter the vector has the humanized *Renilla* luciferase-neomycin resistance cassette (*hRluc-neo*), which is used as a control reporter for normalization of gene expression. The synthetic poly (A) signal acts like a stop site of the transcription. The plasmid contains the Amp gene for bacterial selection for amplification of the vector.

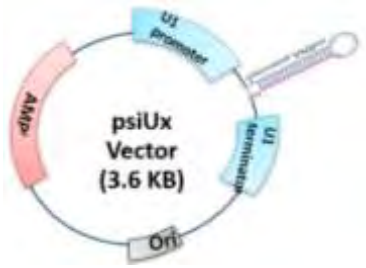

Figure 10 psiUx miRNA overexpression Vector[43]

The miRNA overexpression vector is represented in figure 10.

The vector contains the Amp gene for bacterial selection. The precursor region of the putative microRNAs was cloned under the control of U1 promoter and U1 terminator. The precursors of the miR-181a, miR-615-5p, miR-939. miR-659, miR-608 were cloned inside the vector. Through the use of this overexpressing vector we have a physiological production of the mature miRNA inside the cell.

Finally, the AAV- GFP vector was used in order to validate the transfection efficiency and efficacy through Operetta®.

5.2. Eukaryotic cell line

In our study, in order to examine the mechanism of the post- transcriptional regulation in *GRN* we use HeLa cell lines.

HeLa cells are derived from human cervix. They are adenocarcinoma cell line. HeLa cells are cultured in complete Dulbecco's Modified Eagle's Medium (DMEM). The complete DMEM contains DMEM with 4.5% g/L Glucose (GIBCO) supplemented with 10% Fetal Bovine Serum (FBS), 1% Glutamine and 1% Penicillin- Streptomycin. Cells

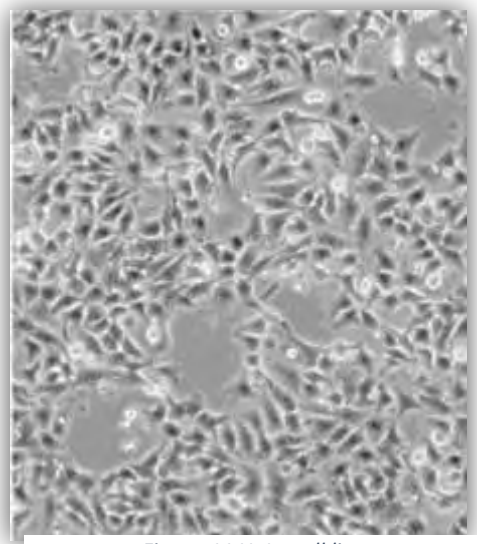

Figure 11 HeLa cell line

are grown and maintained at 37°C with 5% CO_2 in a cell incubator.

5.3. Amplification of the *GRN* 3' UTR and sequencing

We performed RT-PCR in different cell lines, such as HeLa and different types of neuroblastoma cell lines, SH-SY5Y, SK-N-BE, Kelly and CHP212 to amplify the full length 3' UTR of *GRN* of 304bp. The PCR protocol is described below.

Firstly, we had to perform cDNA synthesis (RevertAid First Strand cDNA synthesis, Thermo Scientific) from the RNA extracted from each cell line.

Reagents	
RNA(500ng)	1μL
Oligo(dt) Primer	1μL
H_2O	10μL
Final Volume	12μL

Temperature	Time
65°C	5minutes

Reagents	
Reaction Buffer (5x)	4μL
Riboblock Inhibitor(20u/μL)	1μL
dNTPS Mix (10mM)	2μL
Reverse Transcriptase(200u/μL)	1μL
Final Volume	8μL

Temperature	Time
42°C	60minutes
70°C	5minutes

After we performed amplification of the cDNA with the protocol below.

Reagents	
cDNA	2.5μL
Buffer (10x)	2.5μL
dNTPS (10mM)	0.5μL
Primer Forward (10μM)	0.5μL
Primer Reverse (10μM)	0.5μL
Taq RBC (5unit)	0.25μL
H_2O	18.25μL

Temperature	Time
95°C	1minute
95°C	1minute
54°C	50seconds
72°C	1minute
95°C	5minutes

We used the sequencing service of BMR Genomics to check the 3' UTR of *GRN*. We use 12.2ng of the purified PCR fragment and 3.2μL from each primer. The sequence of the primers that we used is:

Primer Forward: 5'-AATCTAGAGGGACAGTACTGAAG-3'

Primer Reverse: 5'-ATCTAGAGAAAGTGTACAAACTTTATT-3'

5.4. Transfection of Eukaryotic cell lines

5.4.1. Validation of transfection efficiency through Operetta®

In order to validate the transfection efficiency in HeLa cells we transfected them with the AAV-GFP vector. We checked different concentrations of DNA and also different amount of cells. The analysis was done by Operetta® and we choose as better result the 450ng of total DNA and 75.000 cells. The Operetta® is a microplate reader for high content screening. It can acquire, analyze and manage fluorescence and brightfield images. Operetta® has a high power Xenon lamp (300W) providing entire visible spectrum. It has also, 4 or 8 excitation filters and up to 4 automatically

Figure 12 Operetta ®

exchangeable objective lenses for different fields of view/ resolutions.

5.4.2. HeLa cells transfection

Transfection experiments were performed with HeLa cells. The protocol used derived from Invitrogen's manufacturer protocol. 75000 HeLa cells were plated in each well of a 24-well format. We co-transfected HeLa with a 3'UTR of *GRN* reporter vector (pmirGLO) and a miRNA overexpressing vector (psiUx) according to the best transfection efficiency obtained in the Operetta® analysis. The co-transfection were performed with the use of Lipofectamine LTX, a chemical substance that contains lipid subunits that can form liposomes in an aqueous environment, which entrap the transfection materials, such as DNA plasmids. Lipofectamine is a cationic liposome formulation, which complexes with negatively charged nucleic acid molecules to

allow them to overcome the electrostatic repulsion of the cell membrane. The Lipofectamine LTX was combined with Plus Reagent, which is a proprietary reagent for pre-complexing DNA that enhances cationic lipid-mediated transfection of DNA in eukaryotic cells. A dilution of the Lipofectamine LTX Reagent was performed in Opti-MEM medium, using a ratio of 1:3 (µg of DNA: µL Lipofectamine LTX) and the Plus Reagent ratio was 1:1 to the DNA used. Every transfection experiment was done twice in biological duplicates.

For the protein analysis 375000 cells per well were transfected in a 6-well plate with 2µg of miRNAs-overexpressing plasmids and Lipofectamine LTX in a ratio 1:3.

5.5. Analysis of expression

5.5.1. Dual- Glo Luciferase Assay

The Dual-Glo® Luciferase Assay is designed to allow high throughput analysis of mammalian cells containing genes for firefly and *Renilla* luciferases grown in 96- or 384- well plates. The reporter plasmid pmirGLO, contains the firefly luciferase (luc2) that is a 61 kDa protein, used as a primary reporter to monitor the regulation of different miRNAs on the *GRN* 3'UTR and *Renilla* (hRluc) that is a 36 kDa protein used for the normalization. These proteins are monomeric and they don't require post-translational processing. Their function can act immediately upon translation. 35µL of Opti-MEM was added directly to the cells, subsequently 35µL of the Dual-Glo® Luciferase Assay Reagent (LAR) was added to each well. This reagent induces the cell lysis and act as a substrate for firefly luciferase.

Table 1 Composition of RIPA Buffer

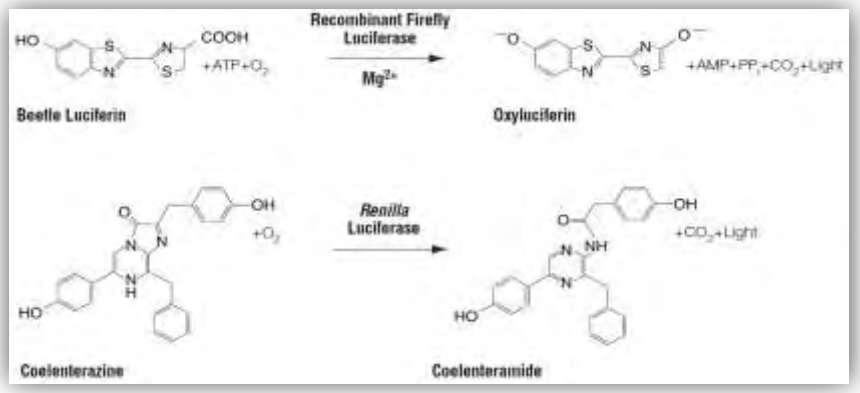

Figure 13 Diagram of firefly and Renilla luciferase reactions with their respective substrates, beetle luciferin and coelenterazine, to yield light.

The plate was wrapped in an aluminium foil to preserve the LAR reagent from light and incubated for 15 minutes at room temperature in a shaking Thermoblock. Subsequently, 20µL of lysate were loaded in a 384-well plate in technical triplicates and used for the measurement of the firefly luminescence on Infinite M200 Tecan multiwell plate reader. Then 20µL of the Dual-Glo® Stop & Glo® Reagent diluted in a ratio of 1:100 were added directly to the 384-well plate to block the firefly luciferase and allow the detection of the *Renilla* Luciferase, incubated at 25 ^{o}C for 30 minutes and then measured on the Infinite M200 Tecan multiwell plate reader.

As represented in figure 14, after the co-transfection with pmirGLO and psiUx in HeLa cells if there is no specific miR that binds in the 3'UTR of the interest there is a consistent signal of luciferase production. If there is a specific miR that binds to the

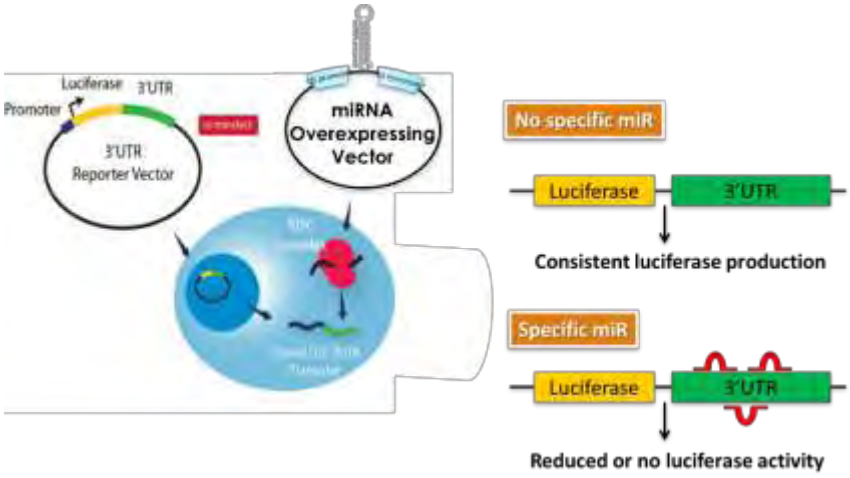

Figure 14 Scheme of the luciferase- based reporter system for miRNA- 3'UTR interaction

3' UTR there is a reduction of luciferase activity.

5.5.2. Extraction of RNA through Trizol and quantification

After the co-transfection of HeLa cell line with pmirGLO and psiUx the cells were detached from the 24-well using 50µl of trypsin that is then inactivated through the use of a DMEM medium containing FBS (Fetal Serum Bovine). All the cells were transferred in an eppendorf tube of 1.5ml and centrifuged at 3600rpm, 4^{o}C for 5 minutes in order to have a pellet of cells. Afterwards the supernatant was removed and the cells were kept at -80^{o}C. Trizol Reagent from life technologies was used for RNA extraction. The Trizol Reagent is designed to isolate high quality total RNA from cells. It is a monophasic solution of phenol, guanidine isothiocyanate and other components used to dissolve the cellular components with no damage for the RNA. 100µL Trizol Reagent were added directly to the pellet of cells and lysis of the cells was performed by pipetting up and down. The samples were incubated for 5 minutes at room temperature to permit complete dissociation of the nucleoprotein complex. After centrifugation of the samples at 12000 x g for 10 minutes at 4°C, the cleaned supernatant was transferred to a new tube. 20µL chloroform were added and the samples were shaked vigorously by hand or by vortex for 15 seconds. An incubation took place for 2-3 minutes at room temperature and a centrifugation of the samples at 12000x g for 15 minutes at 4°C. The mixtures separate into a lower red phenol-chloroform phase, an interphase and a colorless upper aqueous phase. The RNA remains exclusively in the aqueous phase. After centrifugation the aqueous phase was removed and placed in a new tube. 50µL isopropanol were added to the aqueous phase and the samples were incubated for 10 minutes at room temperature. After centrifugation at 12000 x g for 10 minutes at 4°C, the supernatant was removed from the tube, leaving only the RNA pellet. Washing of the pellet with 100µl of 75% ethanol, the samples were vortex briefly, and then centrifuged at 7500 x g for 5 minutes at 4°C. The wash was discarded and the RNA pellet was air dried for 5-10 minutes. Finally, the RNA pellet was resuspended in RNAse- free water by passing the solution up and down several times though a pipette tip. As last step the resuspended RNA was quantified by a NanoDrop™ 1000 Spectrophotometer.

The NanoDrop ™ 1000 Spectrophotometer measures 1µL samples with high accuracy and reproducibility. The spectrometer utilizes a patented sample retention technology that employs surface tension alone to hold the sample in place. In addition, the NanoDrop™ 1000 Spectrophotometer has the capability to measure highly concentrated samples without dilution. NanoDrop can measure not only the concentration of the plasmids but it can identify the purity of the samples through

Figure 15 NanoDrop ™ 1000 Spectrophotometer

the calculations of the 260/280 nm and 260/230 nm ratios.

5.5.3. Real- Time PCR for miRNA detection

In order to detect the mature miRNAs derived from the plasmid of our interest, after the transfection of HeLa with miRNA overexpressing vector, we used the TaqMan® MicroRNA Assay. The TaqMan® MicroRNA Assay are designed to detect and quantify mature microRNAs using real-time PCR instruments. TaqMan® MicroRNA Assays offer high- quality quantitative data, has sensitivity and high specificity. It can detect and quantify miRNA over more than six logs of dynamic range and also as little as 1 to 10 ng of total RNA. The assay detects only the mature miRNA, not its precursor, with single-base discrimination. Also, it is a fast and simple methodology because the two- steps protocol takes less than four hours.

This method consists in two main steps: the first step is a reverse transcription and the second step is a PCR. In the reverse transcription (RT) step, cDNA is reverse transcribed from total RNA samples using specific miRNA primers from the TaqMan® MicroRNA Assays and reagents from the TaqMan® MicroRNA Reverse Transcription

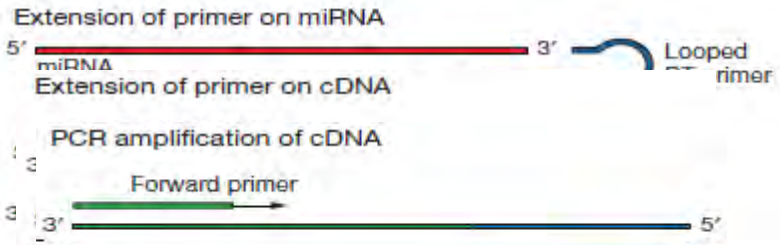

Figure 18 PCR step

Kit.

In the PCR step, PCR products are amplified from cDNA samples using the TaqMan MicroRNA Assay together with the TaqMan® Universal PCR Master Mix. In Table 1 we report a scheme of the protocol followed for the reverse transcription step.

Reagents	RT-PCR Master Mix (µL)
100mM dNTPS (with TTP)	0.15
Multiscribe™ Reverse Transcriptase 50U/µL	1.00
10X Reverse Transcription Buffer	1.50
RNAse Inhibitor 20U/µL	0.19
Nuclease- free water	4.16
RNA 2ng/µL	5.00
Primers	3.00

Time	Temperature
30min	16°C
30min	42°C
5min	85°C
∞	4°C

Table 1 RT-PCR Master mix first step

Reagents	RT-PCR Master Mix (µL)
TaqMan MicroRNA Assay (20X)	1.00
Retrotranscription Product	1.33
TaqMan 2X Universal PCR Master Mix	10.00
Nuclease-free water	7.67

Number Cycles:40	
5min	95°C
15min	95°C
60sec	60°C
∞	4°C

Table 2 RT-PCR Master Mix second step

During the second amplification step, it is possible to record the fluorescent signals generated by the cleavage of TaqMan probes. The final volume of this reaction step is 20µL. The protocol is described in Table 2. Results are analyzed through $2^{-\Delta\Delta Ct}$ method that allows to calculate the relative variation of the expression of a target gene compared to a control gene. The assumption is that real-time PCR achieves optimal amplification efficiencies for both the target and the reference gene. Under these conditions it is possible to define Ct as the threshold value of the PCR reaction. This value is inversely proportional to the logarithm scale of the starting quantity of template cDNA. Moreover, ΔCt is the Ct value for any sample normalized to the endogenous housekeeping gene, while ΔΔCt corresponds to the difference between the average ΔCt value of the target gene and the average ΔCt for the corresponding control gene. Thus, ΔΔCt method provides a sensitive and quantitative measure of

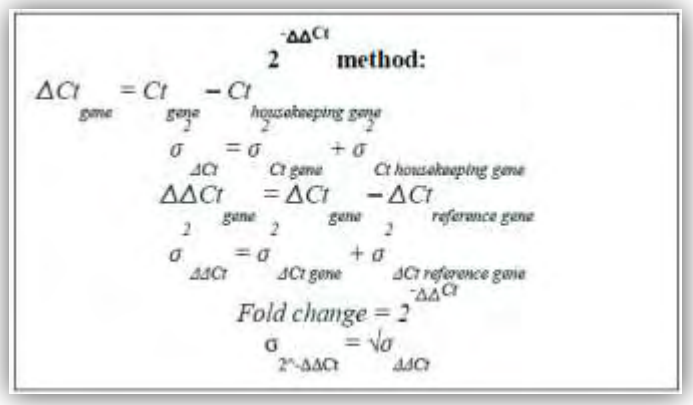

mRNA levels.

5.5.4. Protein extraction and quantification

Transfected HeLa cells derived from a 6-well format, were washed with PBS. Then 150µL of RIPA Buffer and 1x Protease Inhibitors were added.

RIPA Buffer	
Tris HCl (pH=8)	50mM
NaCl	150mM
Protease Inhibitor	1%
NP-40	1%
Sodium Deoxycholate	0.5%

SDS	0.1%

The lysed cells were maintained under constant stirring for 30 minutes at 4^{o}C. We centrifuged the samples at 4^{o}C, 12000rpm for 20 minutes. The supernatant was transferred to a new tube and stored at -80 ^{o}C.

Table 3 Composition of RIPA Buffer

The concentrations of the samples were determined with an Infinite M200 Tecan multiwell plate reader and the Pierce™ BCA Protein Assay Kit, a detergent-compatible formulation based on bicinchoninic acid (BCA) for the colorimetric detection and quantitation of total protein in the samples. In this method, the Cu^{+2} is reduced to Cu^{+1} by protein molecules in the alkaline solution with the highly sensitive and selective colorimetric detection of the cuprous ion (Cu^{+}) using a unique reagent containing bicinchoninic acid with the formation of an intense purple color. This water-soluble complex exhibits a strong absorbance at 562nm that is nearly linear with increasing protein concentrations over a broad working range (20-2000µg/mL). Protein concentrations generally are determined and reported with reference to standards of a common protein such as bovine serum albumin (BSA). A series of dilutions of known concentration are prepared from the protein and assayed alongside the unknown(s) before the concentration of each unknown is determined based on the standard curve.

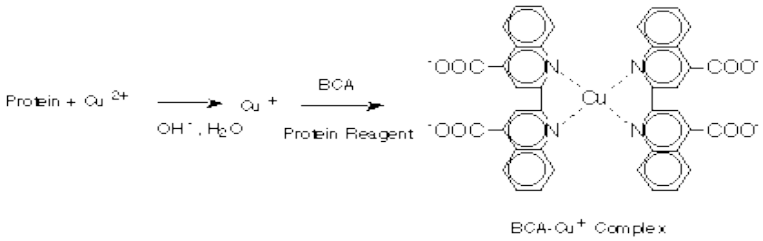

Figure 19 Reaction of BCA protocol

5.5.5. ELISA

In order to quantify the endogenous amount of progranulin protein after the overexpression of the putative microRNAs in a 6-wells format, we used the Progranulin (human) ELISA kit from Adipogen™. This assay is a sandwich Enzyme Linked- Immunosorbent Assay (ELISA) for quantitative determination of human progranulin in biological fluids. A polyclonal antibody specific for progranulin has been precoated onto the 96-well microtiter plate. Standards and samples are pipetted into the wells for binding to the coated antibody. After extensive washing to remove unbound compounds, progranulin is recognized by the addition of a

biotinylated polyclonal antibody specific for progranulin (Detection Antibody). After removal of excess biotinylated antibody, HRP-labeled streptavidin (Detector) is added. Following a final washing, peroxidase activity is quantified using the substrate 3,3',5,5'- tetramethylbenzidine (TMB). The intensity of the color reaction is measured at 450nm after acidification and is directly proportional to the concentration of progranulin in the samples.

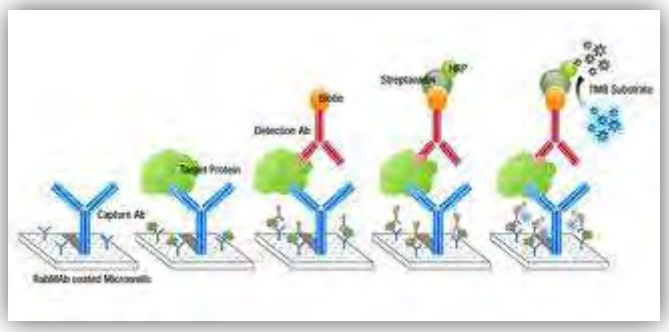

Figure 20 Schematic presentation of Sandwich Elisa

5.5.6. Western Blot

In order to analyze the endogenous levels of progranulin and also the effect of the post-transcriptional regulation of the miRNAs we performed Western Blot assays. After the lysis of the samples, the proteins were separated on a polyacrylamide gel by electrophoresis. This type of running usually takes the name of SDS- PAGE. The gel consists of two parts, the stacking gel and the running gel.

- **Stacking gel** (top of the gel) which allows the proteins in a loaded sample to be concentrated into a tight band during the first few minutes of electrophoresis before entering the resolving portion of a gel.

Stacking gel (4%)	
ddH_2O	1.95ml
Tris-HCl 1.5M (pH=6.8)	205µL
SDS 10%	50µL
Acrylamide/ Bisacrylamide 29:1 30%	350µL
APS 10%	25µL
TEMED	2.5µL
Total	2.5µL

Table 4 Composition of Stacking gel

- **Running gel** (bottom of the gel) which allows the separation of the proteins according to their molecular weight.

Running gel (7.5%)	
ddH_2O	2.4ml
Tris-HCl 1.5M (pH=8.8)	1.25ml
SDS 10%	50µL
Acrylamide/ Bisacrylamide 29:1 30%	1.25ml
APS 10%	25µL
TEMED	2.5µL
Total	5ml

Table 5 Composition of Running gel

The gel is composed of various solutions including SDS, an anionic detergent. It is applied to protein sample to linearize proteins and to impart a negative charge to linearized proteins. The binding of SDS to the polypeptide chain imparts an even distribution of charge per unit mass, thereby resulting in a fractionation by approximate size during electrophoresis. APS and TEMED are essential to initiate the polymerization. The proteins, after the addition of the loading dye, are denatured at 95^{o}C for 5minutes. The voltage was kept constant at 90V until the end of the stacking gel and then the voltage was set at 180V.

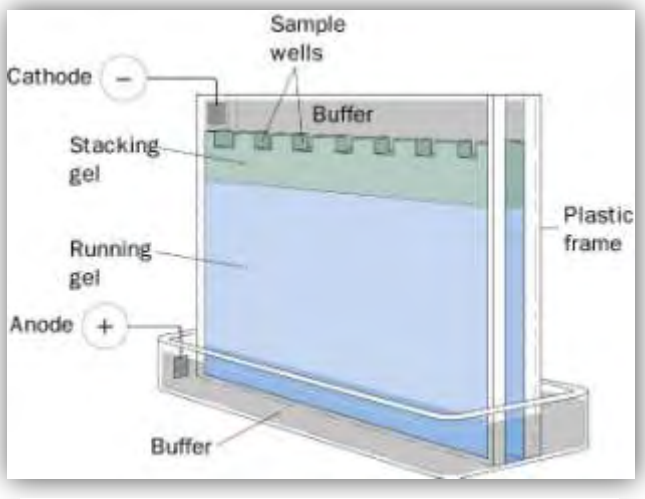

Figure 21 SDS-PAGE

Once the gel was over, we transferred the proteins on a nitrocellulose membrane using the system of iBlot (Invitrogen), an instrument for dry transfer that requires only 7 minutes at 20V. After the transfer to the membrane, the proteins were visualized using Ponceau red. Ponceau is used to prepare a stain for rapid reversible detection of protein bands on nitrocellulose membranes. After the membrane was washed several times with ddH_2O. The membrane was placed for few hours with 5% milk in PBS-T at room temperature. Then, after the blocking the membrane was incubated overnight at 4^{o}C in a diluted solution (1:5000) of primary rabbit monoclonal antibody to GRN (ab108608, Abcam®) in 2% milk in PBS-T. The membrane was washed 3 times with PBS-T and then incubated with the secondary antibody (926-32211 IRDye® 800CW Goat anti-Rabbit) diluted in milk powder 1% in PBS-T. The secondary antibody (IRDye) specifically recognizes the primary antibody bound to the target protein. In particular the secondary antibody reacts with the light chains of rabbit IgM and IgA. IRDye infrared secondary antibody is optimized for high sensitivity and excellent signal to noise performance on LI-COR imaging system. LI-COR's laser technology and 800nm channel were used for the detection of the Western Blot image. HPRT was used as a reference gene to normalize the results using an anti-HPRT monoclonal rabbit antibody (sc-20975, Santa Cruz Biotechnology®) and detected with the same secondary antibody (926-32211 IRDye® 800CW Goat anti-Rabbit).

6. Results

6.1. Validation of the transfection efficiency

In order to validate the transfection efficiency in HeLa cells we used Operetta®. We analyzed different amounts of total DNA (300 ng, 400 ng, 500 ng and 600 ng) and also different amounts of cells per well (65000 cells, 75000 cells and 85000 cells) in a 24-well plate. We used the AAV-GFP vector and Lipofectamine LTX to transfect HeLa cells, and we checked vitality and the efficiency at 24h and 48h after transfection. From the Operetta® analysis the best concentration of total DNA is 450 ng and the best amount of cells is 75000 cells for 24-well plate at 24h and 48h. The efficiency at 24h was around 30% and at 48h was around 65%, as measured calculating the number of GFP- positive cells over the total number of cells. The mortality rate compare the not treated cells was around 40%. Figures 22-25 show representative images from Operetta® at 24h or at 48h post-transfection.

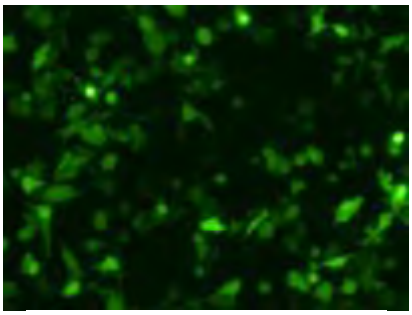

Figure 22 Operetta® analysis 24h, 400ng, 75.000cells

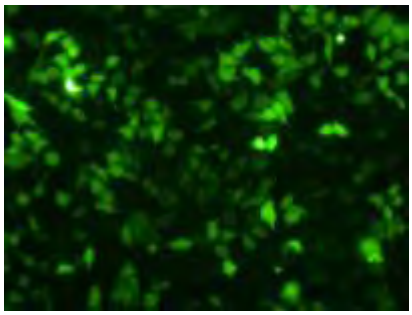

Figure 23 Operetta® analysis 48h, 400ng, 75.000cells

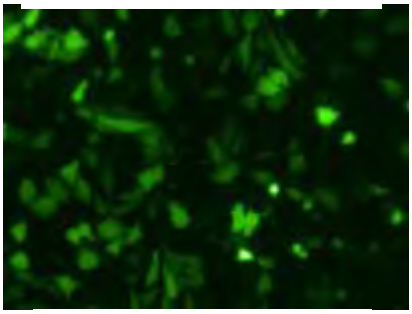

Figure 24 Operetta® analysis 24h, 500ng, 75.000cells

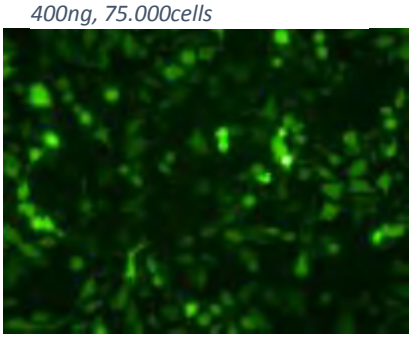

Figure 25 Operetta® analysis 48h, 400ng, 75.000cells

6.2. Analysis by luciferase reporters of miRNA-mediated translational repression

To validate the predicted interaction of miR-608, miR-615-5p, miR-659 and miR-939 with the human *GRN* mRNA 3'UTR, we performed luciferase assay on reporter vector in which luciferase cDNA have been fused to either the full length of 3'UTR or derivatives thereof. The results from the firefly luciferase assays were normalized on the signal of *Renilla* luciferase. The miRNAs under study were produced by transfecting psiUx-based overexpressing vectors. miR-181a was our negative control, because it is not predicted to bind on *GRN* 3'UTR. P-value was calculated using unpaired t-test of three biological experiments. One asterisk (*) means P-value less than 0.05, two asterisks (**) mean P-value less than 0.01 and three asterisks (***) mean P-value less than 0.001.

6.2.1. RNA extraction and quantification and Real Time PCR analysis of miRNA levels

In order to clarify the effect of the over-expressing plasmid used in the luciferase co-transfection experiments we extracted the RNA with Trizol and quantified our samples through NanoDrop ™ 1000 Spectrophotometer.

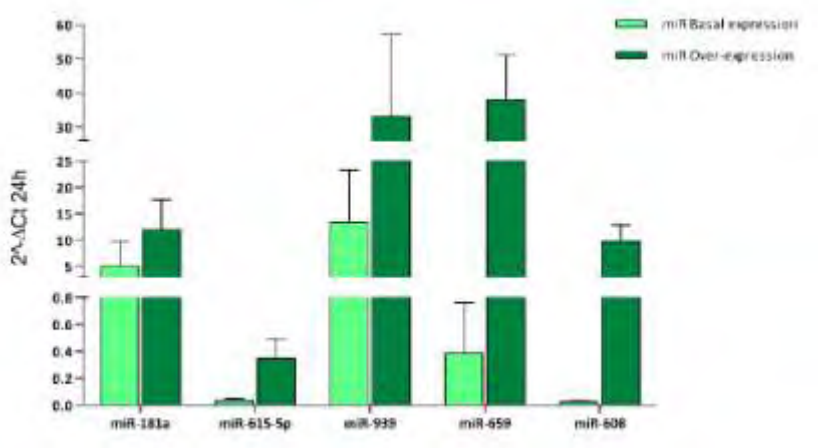

Figure 26 Relative levels of the over-expression of different miRNAs at 24h, with the calculation of $2^{-\Delta Ct}$.

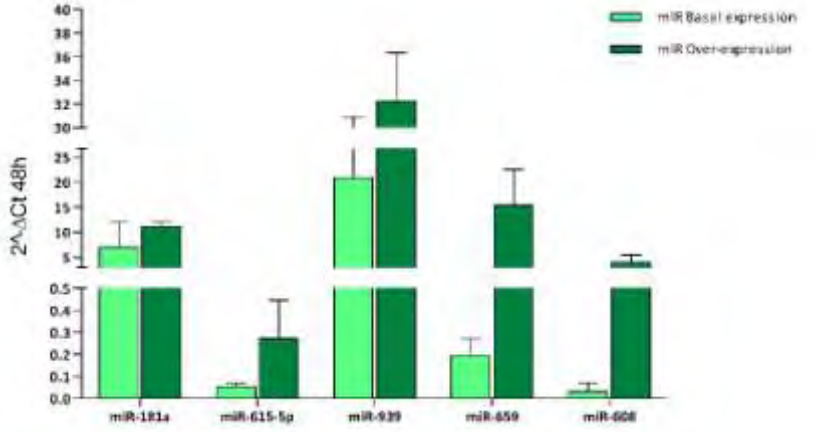

Figure 27 Relative levels of the over-expression of different miRNAs at 48h, with the calculation of $2^{-\Delta Ct}$.

To measure the levels of specific miRNAs we used the TaqMan® MicroRNA Assay. Figures 26 and 27 show the results expressed in $2^{-\Delta Ct}$, a calculation method that allows to visualize the relative levels of the different miRNAs, in the different samples. ΔCt is the Ct value for any sample normalized to the endogenous housekeeping gene. To calculate the fold change of each miRNA upon overexpression, compared to basal levels in mock-transfected cells, results were also analyzed through $2^{-\Delta\Delta Ct}$ method. ΔΔCt corresponds to the difference between the average ΔCt value of the experiment and the average ΔCt for the negative control (cells transfected with empty control plasmid). Figures 28 and 29 show the level of mature microRNAs expressed as fold change ($2^{-\Delta\Delta Ct}$), compared to the basal endogenous levels of microRNAs, averaged on 4 experiments, 24h and 48h after transfection, respectively.

In those graphs light green columns represent the over-expression levels of miR-181a, miR-615-5p, miR-939, miR-659 and miR-608 at basal conditions and dark green columns represent the endogenous levels of miR-181a, miR-615-5p, miR-939, miR-659 and miR-608 after the transfection of the miRNA over-expression vector at 24h and 48h. As we can observe, miR- 181a and miR-939 present at basal condition at 24h and 48h good expression levels inside the cells and they don't show a higher increase upon the over-expression conditions. On the other hand, miR-615-5p, miR-659 and miR-608 show low endogenous expression levels in HeLa cells at basal condition but an higher increases after the over-expression.

Figure 28 Fold change of the over-expression for different miRNAs at 24h

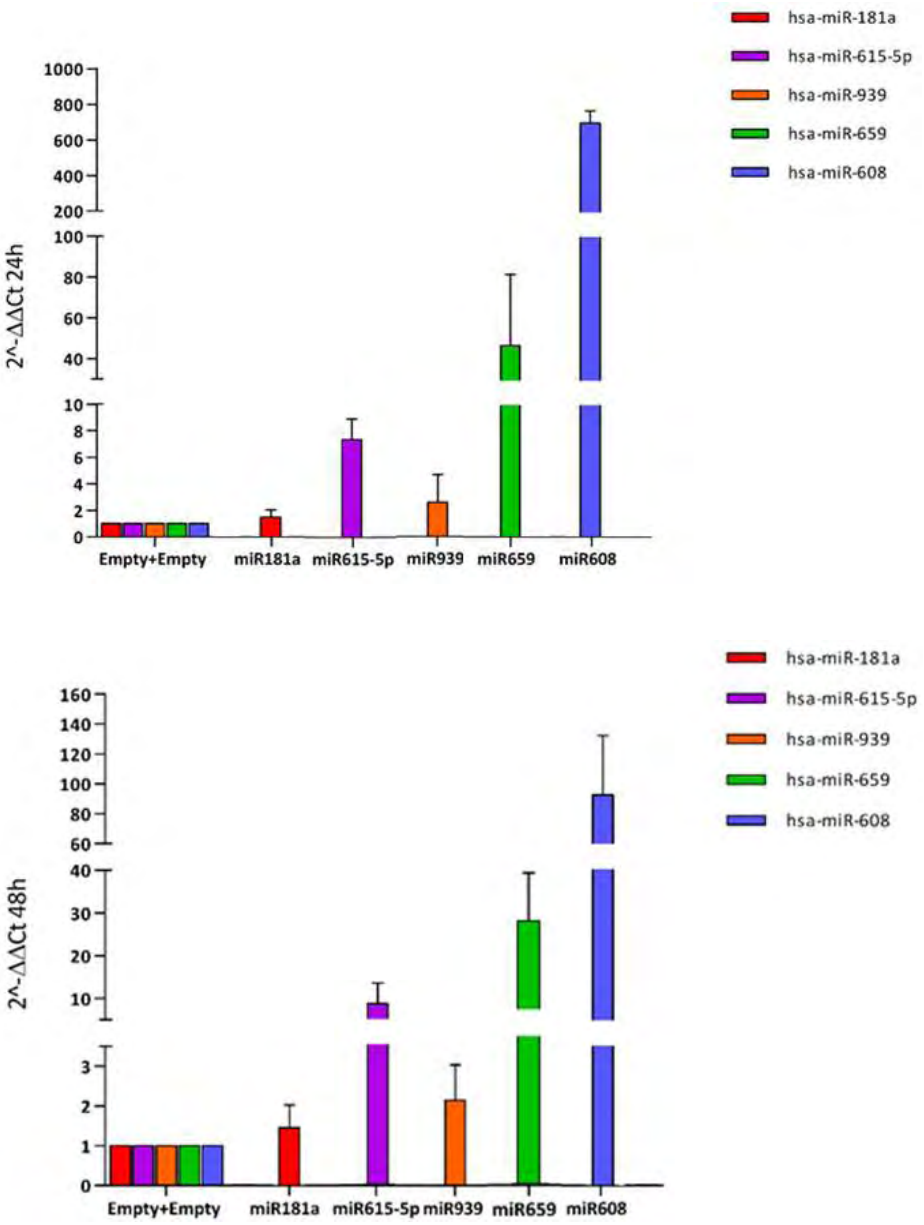

Figure 29 Fold change of the over-expression for different miRNAs at 48h

The graphs show at 24h an increase in the levels of production of the mature miR-615-5p (7.7-fold), miR-659 (47-fold) and miR-608 (697-fold) compared to the basal levels observed in the presence of the empty psiUx plasmid, whereas the over-expression of miR-939 (2.5-fold) and miR-181a is lower (1.5-fold), since the two microRNAs have a higher level of expression at normal/basal condition in HeLa cells.

Regarding the over-expression reached at 48 hours, it is interesting to note that while it is slightly higher for miR-615-5p, compare to 24 hours, for the others miRNAs there seems to be no accumulation over time of the microRNAs. In particular, miR-181a and miR-939 seem to keep the same over-expression levels at 24h and 48h,

while miR-608 and miR-659 over-expression decreases over time, displaying at 48h respectively 1/6 and half of the levels reached at 24 hours.

6.2.2. miR-608, miR-615-5p, miR-659 and miR-939 interact with *GRN* full length 3'UTR

After co-transection of HeLa cells with a pmirGLO vector, containing the full length *GRN* 3'UTR, and psiUx vectors, over-expressing miR-181a, miR-615-5p, miR-939, miR-659 or miR-608 we performed luciferase assays in order to investigate putative interactions between the microRNAs and the *GRN* 3'UTR, at 24h and at 48h.

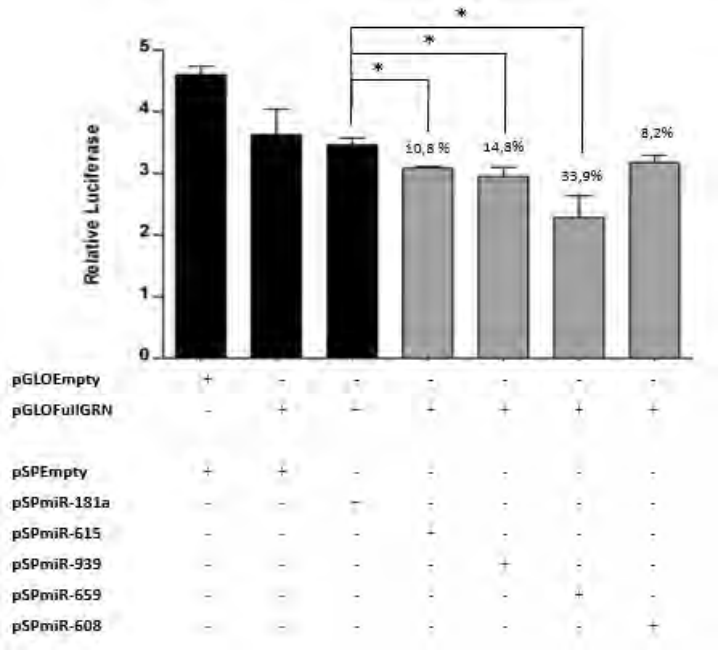

Figure 30 Results from Luciferase assay 24h full length GRN 3'UTR

Figure 30, shows the relative luciferase measured after 24h. All the analyzed miRNAs have a down-regulation effect of the luciferase activity, compared to the control miR-181a, albeit the luciferase down-regulation measured upon over-expression of the miR-608 does not reach significance. Therefore, the four miRNAs might to play a role on the post-transcriptional regulation of *GRN* 3'UTR. The strongest effect on the regulation of *GRN* 3'UTR is observed with the overexpression of miR-659 with a reduction of 33.9% compared to the luciferase levels obtained upon over-expression

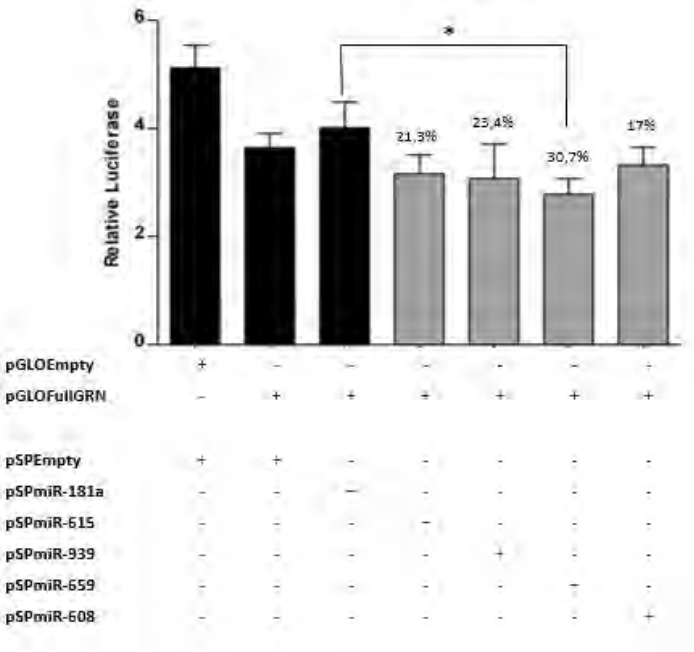

Figure 31 Results from Luciferase assay 48h full length GRN 3'UTR

of control miR-181a.

Figure 31 represents luciferase activity 48 hours after transfection of the plasmids. For all the miRNAs there is an increased effect of downregulation compared to the 24h, indicating the active presence of the mature miRNAs after 48h. However the variability represented as standard deviation increases with a reduction in the significativity of the P-values. The strongest effect on the regulation of *GRN* 3'UTR is again observed with the overexpression of miR-659 with a reduction of 30.7% compare to miR-181a.

6.2.3. miR-608, miR-659 and miR-939 interact with the first 114 bp part of *GRN* 3'UTR

In order to investigate the specific binding sites of different miRNAs on *GRN* 3'UTR, we used a smaller part of the *GRN* 3'UTR in HeLa cells. We performed a co-transfection using the pmirGLO vector, containing the first part of *GRN* 3'UTR (Part I, 114bp), and psiUx vectors over-expressing, miR-181a, miR-615-5p, miR-939, miR-659 or, miR-608. We performed luciferase assay at 24h and at 48h after transfection. From the prediction analysis we expect that Part I of *GRN* 3'UTR could be bound by miR-615-5p, miR-939 and miR-608 on two putative binding sites for each and by miR-659 on one single binding site (see Figure 8).

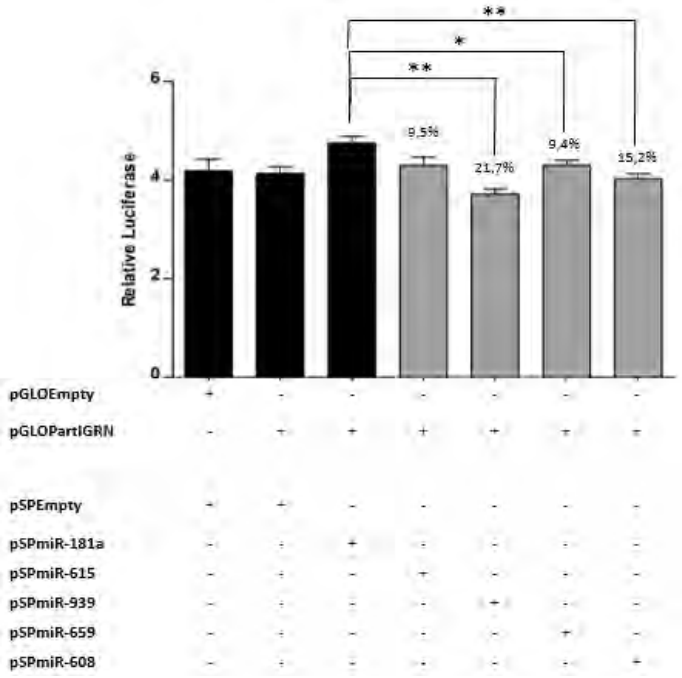

Figure 32 Results from Luciferase assay 24h Part I of GRN 3'UTR

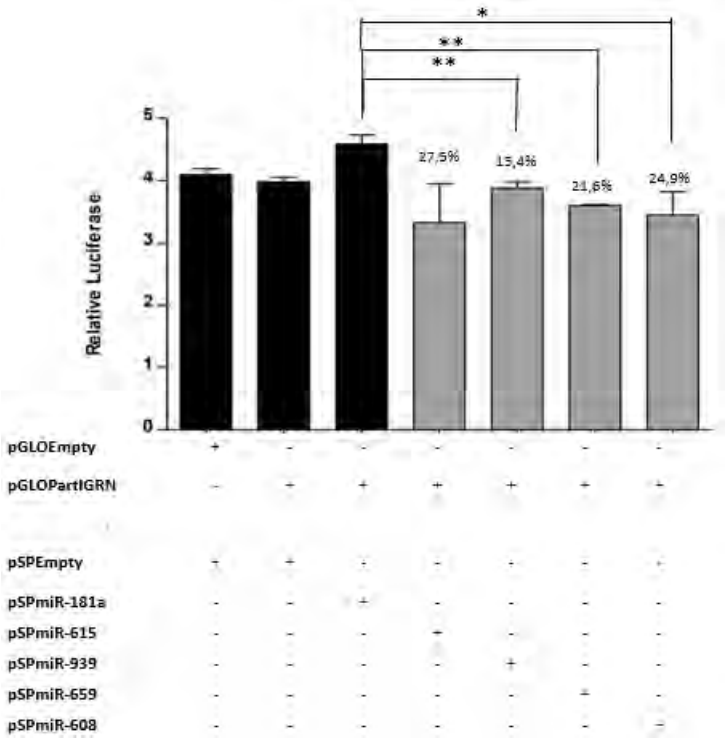

Figure 33 Results from Luciferase activity 48h Part I of GRN 3'UTR

Figure 32, represents the luciferase activity after 24h. Three miRNAs (miR-939, miR-

659, and miR-608) show a significant repression of luciferase activity. The strongest effect is observed with the overexpression of miR-939 with a reduction in luciferase levels of 21.7% compared to miR-181a levels, whereas miR-615-5p induces a small and not significant downregulation of the luciferase.

Figure 33 illustrates the luciferase activity observed after 48h. As for the full-length 3'UTR, there is an increased downregulation for miR-659 and miR-608, compared to the results obtained at 24h. However, upon over-expression of miR-939, a smaller luciferase repression is observed at 48h, compared to 24h.

The downregulation of luciferase observed in Figure 33 with miR-615-5p reaches a reduction of 27.5% compared the negative control with miR-181a. However this reduction is not significant due to the high variability observed during the different experiments. Taken together, these results might indicate that the effect of miR-615-5p, seen on the full length 3'UTR at 24h (Figure 30) might be played through the third binding site of miR-615-5p, localized on the second part of *GRN* 3'UTR.

6.2.4. Does miR-615-5p interact with the first 65nt portion of *GRN* 3'UTR?

In order to better analyze the microRNAs regulation on Part I of *GRN* 3'UTR, we performed a co-transfection experiment in HeLa cells with the pmirGLO vector, containing the first 65bp of *GRN* 3'UTR, dubbed "Fragment A". Fragment A contains only a single binding site for miR-615-5p (see Figure 8) and we did a Luciferase assay in order to investigate only its interaction with miR-615-5p, using miR-181a as a

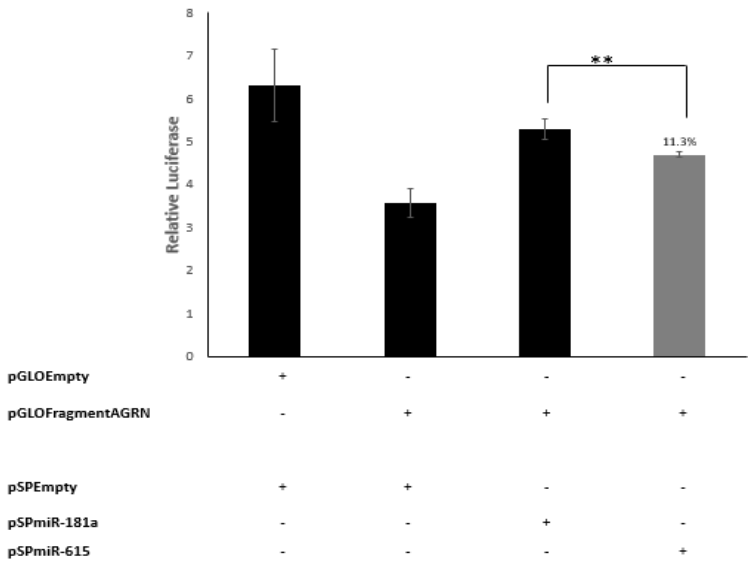

Figure 34 Results from Luciferase activity 24h Fragment A, Part I GRN 3'UTR

negative control.

In figure 34 are reported the results of the luciferase after 24h. In the presence of miR-615-5p there is a small reduction of luciferase of 11.3% compared to the negative control. However this graph reports the results from a single experiment performed at only 24h. Further analysis should include repetitions of this experiment, to be done with the presence of all putative microRNAs under investigation, and also at 48h after transfection.

6.2.5. miR-608, miR-659 and miR-939 interact with portion 60 to 123 nt of *GRN* 3'UTR

Fragment B, corresponding to nt 60 to 123 of *GRN* 3'UTR, contains two binding sites for miR-939 and miR-608, partially overlapping, one binding site for miR-659 and one for miR-615-5p (Figure 8). These interactions were analyzed through co-transfection of HeLa cells with the pmirGLO vector, containing the Fragment B, and the psiUx vectors over-expressing miR-181a, miR-615-5p, miR-939, miR-659 or miR-608. We

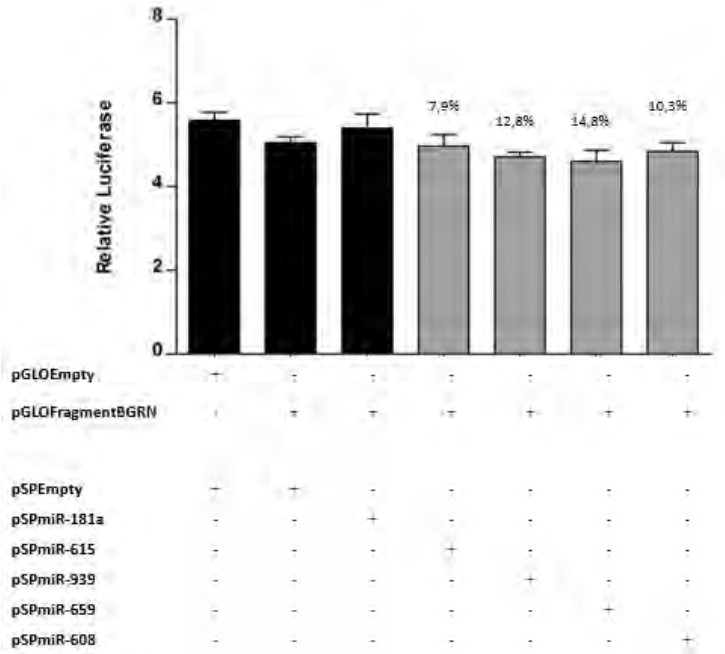

Figure 35 Results from Luciferase activity 24h Fragment B, Part I GRN 3'UTR

performed Luciferase assays at 24h and at 48h.

Figure 35 shows the results after 24h: a small and non-significant downregulation for all the putative miRNAs can be observed.

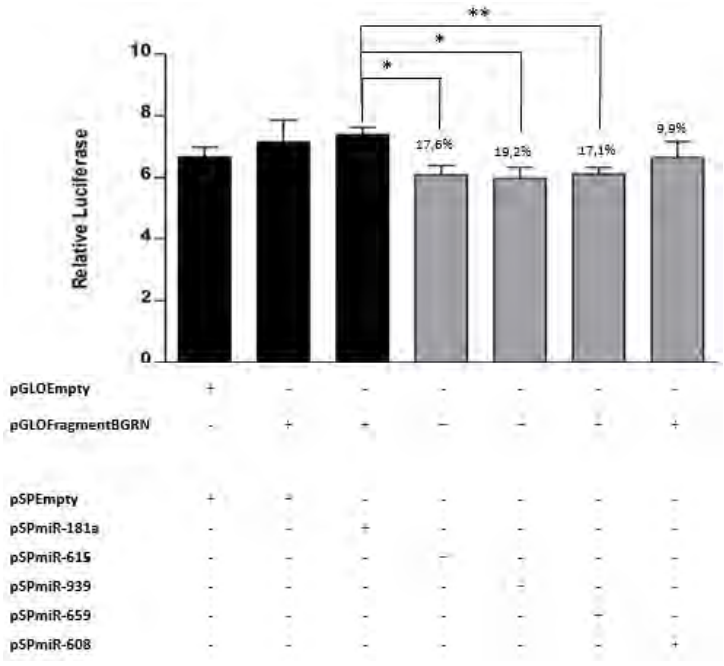

Figure 36 Results from Luciferase activity 48h, Fragment B Part I GRN 3'UTR

The downregulation reported at 24h increases at 48h, as shown in Figure 36. Three microRNAs have a significant effect on luciferase levels at 48h (miR-615-5p, miR-939 and miR-659). As miR-608 and miR-939 have overlapping binding sites, the lack of an effect of miR-608 on the luciferase levels might be due to the higher endogenous level of expression of miR-939 in HeLa cells compared to miR-608.

Overall, we would expect that a small fragment such as Fragment B would be less affected by the endogenous proteins or miRNAs present inside the cells, compare to the full length *GRN* 3'UTR, therefore allowing to observe a higher extent of effect upon over-expression of specific miRNAs. However, we observed a better down-regulation of luciferase with the use of the full-length *GRN* 3'UTR. It can be speculated that the different folding structures of *GRN* 3'UTR and its fragments could play a role on the dynamics of the miRNA interactions and regulations.

6.2.6. The putative interaction of miR-615-5p with the 3' 190-nt portion of *GRN* 3'UTR is not clarified

The 190 bp-long 3' part of *GRN*, dubbed Part II, was analyzed through a Luciferase assay in which we co-transfected HeLa cells with the pmirGLO vector, containing PartII, and psiUx vectors, overexpressing miR-181a, miR-615-5p, miR-939 or miR-608. Part II includes only a predicted binding site for miR-615-5p.

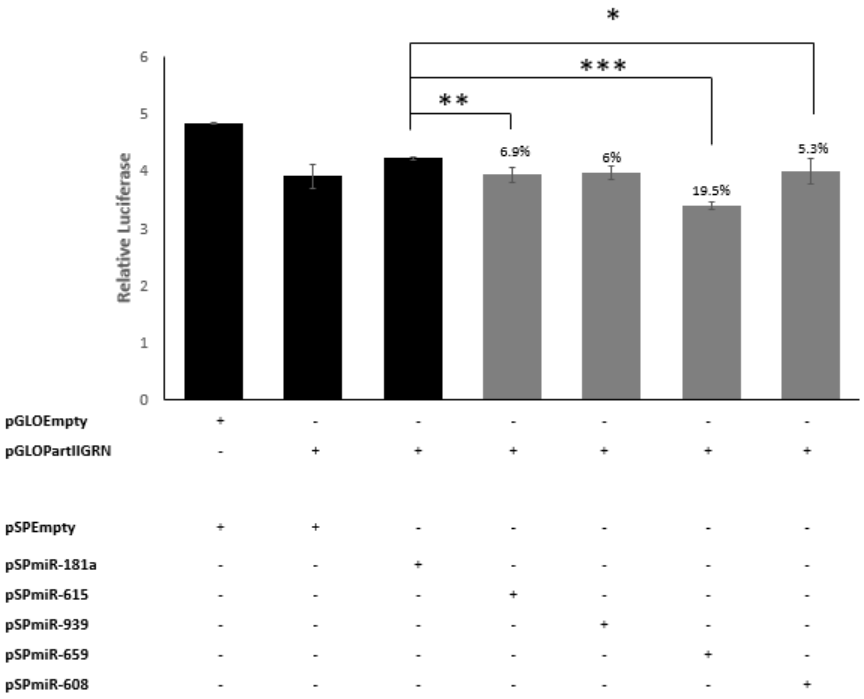

Figure 37 Results from Luciferase activity 24h Part II of GRN 3'UTR

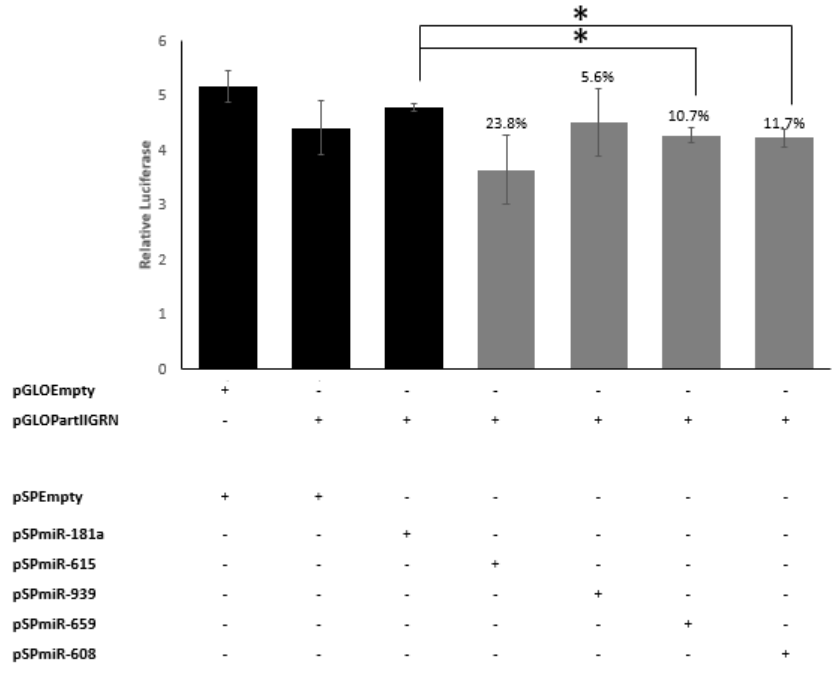

Figure 38 Results from Luciferase activity 48h Part II of GRN 3'UTR

Figure 37 illustrates the result of luciferase assays after 24h. Unexpectedly, the strongest

effect o Part II *GRN* 3'UTR is observed upon over-expression of miR-659, with a reduction of 19.5% compare to miR-181a, even without the presence of predicted binding sites for miR-659 on this part of *GRN* 3'UTR. However, this graph reports the results from a single experiment performed at 24h and 48h. Further analysis should include repetitions of this experiment, in order to understand this down-regulation of luciferase, when over-expression of miR-659 took place.

However, this effect of miR-659 is reduced at 48h, as we can observed from Figure 38. As expected the Figure 38 shows a major reduction of luciferase of 23.8% with miR-615-5p compare the negative control. This results derive from a single experiment with two biological duplicate and three technical replicates. Therefore further experiments should be performed to confirm and better investigate on the miRNA regulation of the Part II of *GRN* 3'UTR.

6.3. miR-608 and miR-659 regulate endogenous progranulin levels

6.3.1. ELISA analysis

In order to analyze the effect of the overexpression of our miRNAs of interest on the endogenous progranulin protein level a sandwich Enzyme Linked- Immunosorbent Assay (ELISA) for quantitative determination of human progranulin in biological fluids

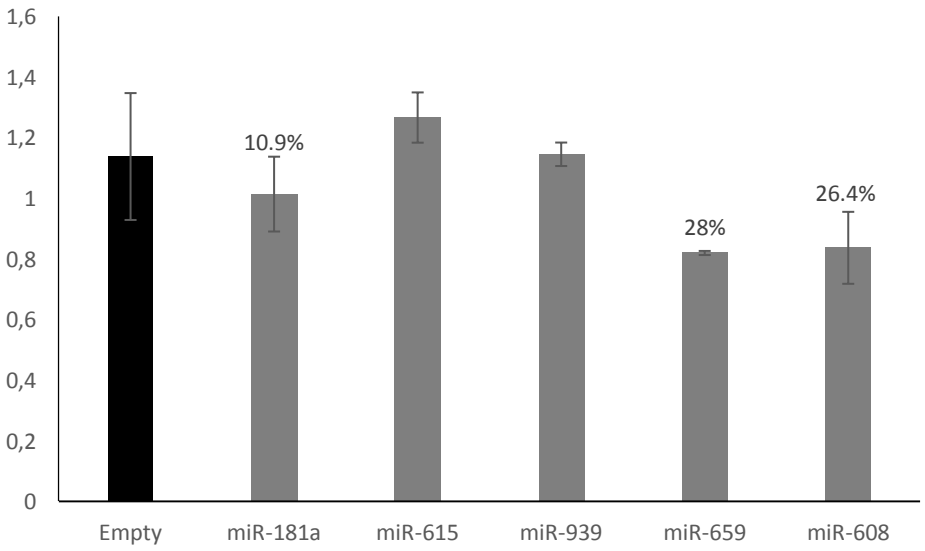

(Adipogen).

Figure 39 shows the ELISA result 48h after transfection of the miRNA over-expressing vectors in HeLa cells. A strong downregulation of progranulin levels were observed with miR-608 (-26.4%) and miR-659 (-28%). A small and not significant down-regulation is also shown in the presence of miR-181a, possibly due to the presence of a potential binding site for miR-181a on the coding region of progranulin. These results derived from a single experiment with 3 technical replicates and further analysis are necessary to confirm these data.

6.4. Western Blot

In order to quantify the endogenous amount of protein after the overexpression of

Figure 39 Results of Elisa assay 48h

the putative microRNAs in 6 well format, using HeLa cells, we used Western Blot. For

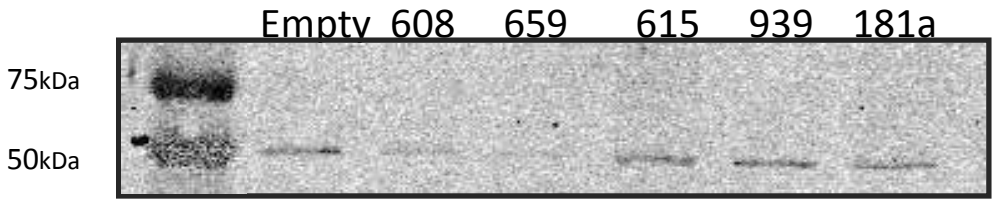

the Western Blot we used 20μg of total protein. The next figures show the results from Western Blot.

miR-659 and miR-608 have the strongest repression effect on the endogenous levels

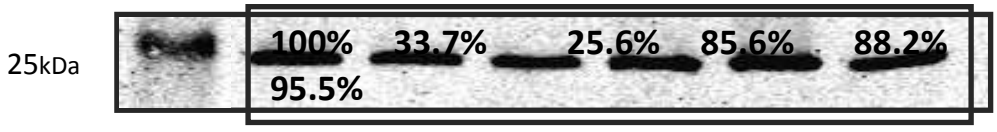

Figure 40 Western Blot results

of progranulin with a percentage of 33.7 and 25.6, compare to the Empty that represent the 100%. Also miR-615 and miR-939 have an effect on the protein level of progranulin, albeit smaller. The strong downregulation of progranulin protein in the presence of miR-659 and miR-608 was therefore confirmed through two different techniques, such as ELISA and Western Blot.

6.5. *GRN* 3' UTR sequencing

We performed an RT-PCR to amplify the full length of *GRN* 3'UTR using RNA extracted from HeLa cells and from four different neuroblastoma cell lines (SH-SY5Y, SK-N-BE, Kelly and CHP212). In order to investigate the presence of polymorphisms in the *GRN* 3' UTR, the RT-PCR reactions were subsequently purified and sent for the sequencing service of BMR Genomics, as described previously. Interestingly we found that three different neuroblastoma cell lines (SK-N-BE, Kelly and CHP212) contain in different proportion the allele of the rs5848 SNP reported by Rademarkers and collaborators[38]. Whereas HeLa and SH-SY5Y cell lines present only the wild type C allele. The sequencing results for the region of interest that contain the SNP are reported in the figures below. As already described, the presence of a SNP creates a stronger binding of the miR-659 that lead to a strong down-regulation and a reduced translation of *GRN* mRNA. Therefore in these cell lines we could potentially aspect to observe a different regulation of the *GRN* mRNA after the over-expression of miR-659, due to the presence or the absence of a common genetic variant localized on the binding site region of miR-659.

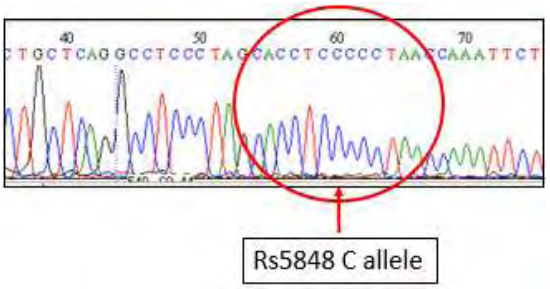

Figure 41 Results from sequencing of HeLa cell line

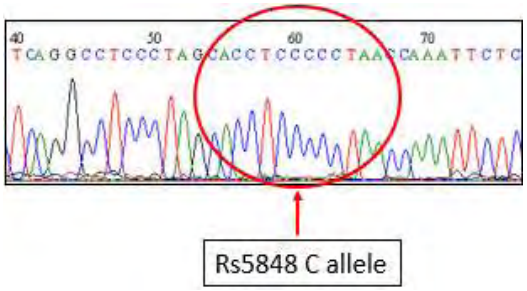

Figure 42 Results from sequencing of SH-SY5Y cell line

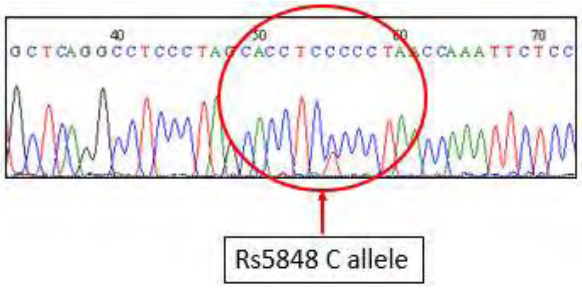

Figure 44 Results from sequencing of CHP212 cell line

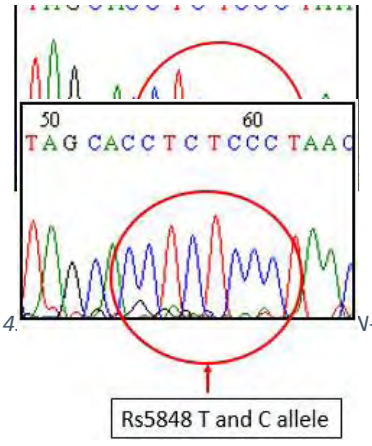

Figure 4 N-BE cell line

Figure 45 Results from sequencing of Kelly cell line

7. Discussion and Future Prospective

Frontotemporal Lobar Degeneration is a neurodegenerative disorder that affects behavior, language and motor skills and can be caused by mutations in several genes such as *GRN*. There is not a unique correlation between the mutations found on the coding region of GRN and the development of the disease. We decided to investigate the regulation of the *GRN* 3'UTR mediated by miRNAs to find if an altered post-transcriptional regulation can be correlated with the pathology. This study is part of a larger project which has as an aim to develop therapeutic strategies for the treatment of the disease. The first aim of this thesis project was to co-transfected the plasmid psiUx and the pGLO vector in HeLa cell line and analyze the miRNAs regulation through Luciferase assay. After the different transfection experiments with all the fragments we observed that the miR-659 has a strong regulation effect on all the fragments and also in the total 3'UTR of *GRN*. We performed Real Time PCR to detect the level of the mature miRNA after the use of the over-expressing vector in HeLa cells. We observed a high level of over-expression for the miR-659, miR-615-5p and miR-608 that show low levels in basal conditions. Whereas miR-181a and miR-939 have a higher endogenous level in HeLa cells and the over-expression was not achieved.The second aim of this study was to check if the miRNAs have any effect on the endogenous levels of progranulin. This question was checked through Elisa Assay and Western Blot. The results from those assays shown that miR-659 and miR-608 have a strong regulation effect on the endogenous levels of progranulin. Further analysis should be done to validate the effect of miR over-expression on the

protein level through Western Blot and ELISA. Also, it would be helpful to use mutations site specific to understand better the role of each microRNAs on the 3'UTR of *GRN*.

8. References

1. Snowden JS. Frontotemporal dementia. *Br J Psychiatry*. 2002;180(2):140-143. doi:10.1192/bjp.180.2.140.

2. Sieben A, Van Langenhove T, Engelborghs S, et al. The genetics and neuropathology of frontotemporal lobar degeneration. *Acta Neuropathol*. 2012;124(3):353-72. doi:10.1007/s00401-012-1029-x.

3. Pan X-D, Chen X-C. Clinic, neuropathology and molecular genetics of frontotemporal dementia: a mini-review. *Transl Neurodegener*. 2013;2(1):8. Available at: http://www.pubmedcentral.nih.gov/articlerender.fcgi?artid=3639184&tool=pmcentrez&rendertype=abstract.

4. Rohrer JD, Lashley T, Schott JM, et al. Clinical and neuroanatomical signatures of tissue pathology in frontotemporal lobar degeneration. *Brain*. 2011;134(Pt 9):2565-81. doi:10.1093/brain/awr198.

5. Cairns NJ, Bigio EH, Mackenzie IRA, et al. NIH Public Access. 2010;114(1):5-22. doi:10.1007/s00401-007-0237-2.Neuropathologic.

6. Rademakers R, Cruts M, van Broeckhoven C. The role of tau (MAPT) in frontotemporal dementia and related tauopathies. *Hum Mutat*. 2004;24(4):277-95. doi:10.1002/humu.20086.

7. Dejesus-hernandez M, Mackenzie IR, Boeve BF, et al. NIH Public Access. 2012;72(2):245-256. doi:10.1016/j.neuron.2011.09.011.Expanded.

8. Cruts M, Theuns J, Van Broeckhoven C. Locus-specific mutation databases for neurodegenerative brain diseases. *Hum Mutat*. 2012;33(9):1340-4. doi:10.1002/humu.22117.

9. Kumar-Singh S, Van Broeckhoven C. Frontotemporal lobar degeneration: current concepts in the light of recent advances. *Brain Pathol*. 2007;17(1):104-14. doi:10.1111/j.1750-3639.2007.00055.x.

10. Weihl CC, Pestronk A, Kimonis VE. NIH Public Access. 2010;19(5):308-315. doi:10.1016/j.nmd.2009.01.009.Valosin-containing.

11. Mackenzie IR, Rademakers R, Neumann M. TDP-43 and FUS in amyotrophic lateral sclerosis and frontotemporal dementia. *Lancet Neurol*. 2010;9(10):995-1007. doi:10.1016/S1474-4422(10)70195-2.

12. Lagier-Tourenne C, Polymenidou M, Cleveland DW. TDP-43 and FUS/TLS: emerging roles in RNA processing and neurodegeneration. *Hum Mol Genet*. 2010;19(R1):R46-64. doi:10.1093/hmg/ddq137.

13. Eriksen JL, Mackenzie IRA. Progranulin : normal function and role in neurodegeneration. 2008:287-297. doi:10.1111/j.1471-4159.2007.04968.x.

14. Chen-plotkin AS, Martinez-lage M, Sleiman PMA, et al. NIH Public Access. 2012;68(4):488-497. doi:10.1001/archneurol.2011.53.Genetic.

15. Gass J, Prudencio M, Stetler C, Petrucelli L. Progranulin: an emerging target for FTLD therapies. *Brain Res*. 2012;1462:118-28. doi:10.1016/j.brainres.2012.01.047.

16. Songsrirote K, Li Z, Ashford D, Bateman A, Thomas-Oates J. Development and application of mass spectrometric methods for the analysis of progranulin N-glycosylation. *J Proteomics*. 2010;73(8):1479-90. doi:10.1016/j.jprot.2010.02.013.

17. Hrabal R, Chen Z, James S, Bennett HPJ, Ni F. The hairpin stack fold, a novel protein architecture for a new family of protein growth factors. *Nat Struct Biol*. 1996;3(9):747-752. doi:10.1038/nsb0996-747.

18. Bateman A, Belcourt D, Bennett H, Lazure C, Solomon S. Granulins, a novel class of peptide from leukocytes. *Biochem Biophys Res Commun*. 1990;173(3):1161-1168. doi:10.1016/S0006-291X(05)80908-8.

19. Xu S, Tang D, Pronk G, et al. CELL BIOLOGY AND METABOLISM : The Granulin / Epithelin Precursor Abrogates the Requirement for the Insulin-like Growth Factor 1 Receptor for Growth in Vitro The Granulin / Epithelin Precursor Abrogates the Requirement for the Insulin-like Growth Factor 1 . 1998.

20. Plowman GD, Green JM, Neubauer MG, et al. The Epithelin Precursor Encodes Two Proteins with Opposing Activities on Epithelial Cell Growth * kidneys based on their ability to inhibit the growth of. 1992.

21. Hoque M, Mathews MB, Pe'ery T. Progranulin (granulin/epithelin precursor) and its constituent granulin repeats repress transcription from cellular promoters. *J Cell Physiol*. 2010;223(1):224-33. doi:10.1002/jcp.22031.

22. Daniel R, Daniels E, He Z, Bateman A. Progranulin (acrogranin/PC cell-derived growth factor/granulin-epithelin precursor) is expressed in the placenta, epidermis,

microvasculature, and brain during murine development. *Dev Dyn*. 2003;227(4):593-9. doi:10.1002/dvdy.10341.

23. Daniel R, He Z, Carmichael KP, Halper J, Bateman a. Cellular Localization of Gene Expression for Progranulin. *J Histochem Cytochem*. 2000;48(7):999-1009. doi:10.1177/002215540004800713.

24. Arai T, Hasegawa M, Akiyama H, et al. TDP-43 is a component of ubiquitin-positive tau-negative inclusions in frontotemporal lobar degeneration and amyotrophic lateral sclerosis. *Biochem Biophys Res Commun*. 2006;351(3):602-11. doi:10.1016/j.bbrc.2006.10.093.

25. Gass J, Cannon A, Mackenzie IR, et al. Mutations in progranulin are a major cause of ubiquitin-positive frontotemporal lobar degeneration. *Hum Mol Genet*. 2006;15(20):2988-3001. doi:10.1093/hmg/ddl241.

26. Cruts M, Gijselinck I, van der Zee J, et al. Null mutations in progranulin cause ubiquitin-positive frontotemporal dementia linked to chromosome 17q21. *Nature*. 2006;442(7105):920-4. doi:10.1038/nature05017.

27. Cruts M, Van Broeckhoven C. Loss of progranulin function in frontotemporal lobar degeneration. *Trends Genet*. 2008;24(4):186-94. doi:10.1016/j.tig.2008.01.004.

28. Baker M, Mackenzie IR, Pickering-Brown SM, et al. Mutations in progranulin cause tau-negative frontotemporal dementia linked to chromosome 17. *Nature*. 2006;442(7105):916-9. doi:10.1038/nature05016.

29. Davis-Dusenbery BN, Hata A. MicroRNA in Cancer: The Involvement of Aberrant MicroRNA Biogenesis Regulatory Pathways. *Genes Cancer*. 2010;1(11):1100-14. doi:10.1177/1947601910396213.

30. Lee Y, Kim M, Han J, et al. MicroRNA genes are transcribed by RNA polymerase II. *EMBO J*. 2004;23(20):4051-60. doi:10.1038/sj.emboj.7600385.

31. Lee Y, Ahn C, Han J, et al. The nuclear RNase III Drosha initiates microRNA processing. *Nature*. 2003;425(6956):415-9. doi:10.1038/nature01957.

32. Lee YS, Nakahara K, Pham JW, et al. Distinct Roles for Drosophila Dicer-1 and Dicer-2 in the siRNA/miRNA Silencing Pathways. *Cell*. 2004;117(1):69-81. doi:10.1016/S0092-8674(04)00261-2.

33. Hutvágner G, Zamore PD. A microRNA in a multiple-turnover RNAi enzyme complex. *Science*. 2002;297(5589):2056-60. doi:10.1126/science.1073827.

34. Chendrimada TP, Gregory RI, Kumaraswamy E, et al. TRBP recruits the Dicer complex to Ago2 for microRNA processing and gene silencing. *Nature*. 2005;436(7051):740-4. doi:10.1038/nature03868.

35. Bartel DP. NIH Public Access. 2013;136(2):215-233. doi:10.1016/j.cell.2009.01.002.MicroRNA.

36. Liu J, Rivas F V, Wohlschlegel J, Iii JRY, Parker R, Hannon GJ. NIH Public Access. 2007;7(12):1261-1266.

37. Barbato C, Ruberti F, Cogoni C. Searching for MIND: microRNAs in neurodegenerative diseases. *J Biomed Biotechnol*. 2009;2009:871313. doi:10.1155/2009/871313.

38. Rademakers R, Eriksen JL, Baker M, et al. Common variation in the miR-659 binding-site of GRN is a major risk factor for TDP43-positive frontotemporal dementia. *Hum Mol Genet*. 2008;17(23):3631-3642. doi:10.1093/hmg/ddn257.

39. Jiao J, Herl LD, Farese R V., Gao FB. MicroRNA-29b regulates the expression level of human progranulin, a secreted glycoprotein implicated in frontotemporal dementia. *PLoS One*. 2010;5(5):e10551. doi:10.1371/journal.pone.0010551.

40. Wang W-X, Wilfred BR, Madathil SK, et al. miR-107 regulates granulin/progranulin with implications for traumatic brain injury and neurodegenerative disease. *Am J Pathol*. 2010;177(1):334-345. doi:10.2353/ajpath.2010.091202.

41. Rabinovici GD, Miller BL. *NIH Public Access*.; 2010:375-398. doi:10.2165/11533100-000000000-00000.Frontotemporal.

42. He L, Hannon GJ. Correction: MicroRNAs: small RNAs with a big role in gene regulation. *Nat Rev Genet*. 2004;5(8):631-631. doi:10.1038/nrg1415.

43. Denti M, Rosa a, Sthandier O, Deangelis F, Bozzoni I. A new vector, based on the PolII promoter for the U1 snRNA gene, for the expression of siRNAs in mammalian cells. *Mol Ther*. 2004;10(1):191-199. doi:10.1016/j.ymthe.2004.04.008.